DM

FCT Fundação para a Ciência e a Tecnologia
MINISTÉRIO DA EDUCAÇÃO E CIÊNCIA

CQM CENTRO DE QUÍMICA DA MADEIRA

Investigation of Possibilities for Detection of Stress Hormones in Loggerhead Sea Turtles by MALDI TOF Mass Spectrometry

MASTER DISSERTATION

Dominika Houdová
MASTER IN APPLIED BIOCHEMISTRY

UNIVERSIDADE da MADEIRA
A Nossa Universidade
www.uma.pt

April | 2021

Investigation of Possibilities for Detection of Stress Hormones in Loggerhead Sea Turtles by MALDI TOF Mass Spectrometry

MASTER DISSERTATION

Dominika Houdová
MASTER IN APPLIED BIOCHEMISTRY

ORIENTATION
Thomas Dellinger

CO-ORIENTATION
Marijana Petković

Investigation of Possibilities for Detection of Stress Hormones in Loggerhead Sea Turtles by MALDI TOF Mass Spectrometry

Master Dissertation

A thesis presented for the degree of
Master in Applied Biochemistry

Dominika Houdová

Supervisor
Thomas Dellinger & Marijana Petković

Centro de Química da Madeira,
Campus Universitário da Penteada, 9000-390 Funchal, Portugal
April 30, 2021

Declaration

I hereby declare that this thesis is the result of my own work, is original and was written by me. I also declare that its reproduction and publication by the University of Madeira will not break any third-party rights and that I have not previously (in its entirety or in part) submitted it elsewhere for obtaining any qualification or degree. Furthermore, I certify that all the sources of information used in the thesis were properly cited.

Funchal, April 30, 2021

Acknowledgements

I would like to thank especially my co-supervisor, Dr. Marijana Petkovic, former Senior Researcher at CQM, for giving me the opportunity to work closely with her, helping me at laboratory, expanding my knowledge and for all her support and guidance within this journey. I am also grateful for the friendship we have built during this journey.

I would also like to thank my supervisor, Prof. Dr. Thomas Dellinger, for his help with turtle captivity, sample collection, ideas and his guidance.

Another thanks goes to CQM, The Madeira Chemistry Centre, who allowed me to work at their facilities and with MALDI TOF MS equipment. Likewise, I would like to thank the University of Madeira for providing me with the possibility to perform my master project and improve my scientific skills and knowledge. I am also grateful to Dr. Rosa Perestrelo for supervising me within MALDI analysis, for her patience and time.

I would also like to express my gratitude to Dr. Manuel Algarra allowing me to participate and contribute to his project "Chemically heterogeneous carbon dots enhanced cholesterol detection by MALDI TOF mass spectrometry" which has been published.

In addition, I would like to thank my partner and family who supported and challenged me during the difficult times.

Abstract

Loggerhead sea turtles (*Caretta caretta*) are the most abundant and widespread sea turtle species in Madeiran waters. The species is considered endangered and is protected worldwide, as they encounter many stressors, whether natural or anthropogenic. Being high in the food chain they serve as effective indicator of marine ecosystem health.

The most common method to evaluate the physiological stress is the measurement of corticosterone (CS) levels in plasma. There are several analytical methods for determination of plasma corticosterone concentrations, however most of them require tedious and complicated procedures. The approach for detection and fast screening of CS in blood of a turtle tested in this work was simple, as MALDI does not require sample derivatization, which is extremely useful for analysis of low sample volumes.

Since MALDI has limitations in analysis of small molecules, cholesterol was used as a model system for development of the method and as well nanomaterials (carbon dots (CDs), N-doped carbon dots (N-CDs) and graphene) were used in order to overcome signal suppression in presence of inorganic salts. It was found that CDs and N-CDs are sensitive to the cholesterol and can be used either alone or in a binary system with 2,5-dihydroxybenzoic acid (DHB) to improve detection. In the presence of NaCl, N-CDs had a better reproducibility of results. Afterwards, CS was subjected to analysis, the linearity, precision and limit of detection and quantification with three organic matrices were investigated. Signal-to-noise ratio of the CS-derived signal was used as parameter for quantification.

In order to achieve better linearity and precision, isotopically labeled corticosterone was added at fixed concentration, as a correction factor. The signal at m/z 347.4 belonging to CS was clearly detected. The lowest measured concentration of CS extracted from plasma that was still detectable by MALDI-TOF MS was 0.04 mg/mL, which is approximately ten times higher than expected CS concentration in a turtles' blood. The results of this work showed that this method has a potential for quantification of CS in turtles' blood, however the sensitivity is low, and the method need further

improvements.

Key words: MALDI TOF MS, corticosterone, turtles, stress hormones, low mass molecules

Resumo

A tartaruga-marinha-comum (*Caretta caretta*) é a espécie de tartaruga marinha mais abundante e comum em águas da Madeira. A espécie é considerada ameaçada e está sob proteção a nível mundial, pois é exposta a vários fatores de stresse, sejam estes naturais ou antropogénicos. Estando numa posição alta da cadeia alimentar, a sua presença serve como um indicador efetivo da saúde dos ecossistemas marinhos.

O método mais comum para avaliar o stresse fisiológico é a medição dos níveis de corticosterona (CS) em plasma. Existem vários métodos analíticos para determinar a concentração de corticosterona em plasma, porém a maioria deles consiste em operações tediosas e complicadas. A abordagem apresentada neste trabalho para a deteção e mensuração rápida é simples – a MALDI não exige que se faça derivatização de amostras o que é extremamente útil para a análise de amostras de baixo volume. Como a MALDI tem limitações em relação à análise de pequenas moléculas, foi usado colesterol como o sistema modelo para desenvolver o método, bem como nanomateriais (pontos de carbono (CD), pontos de carbono enriquecidos/dopados com nitrogénio (N-CD) e grafeno) para resolver a supressão de sinais na presença de sais inorgânicos.

Foi constatado que os CD e N-CD reagem ao colesterol e podem ser usados ou individualmente ou num sistema binário com o ácido gentísico (DHB) para melhorar a sua deteção. Foi obtida uma melhor reprodutibilidade de resultados usando N-CD na presença de NaCl. Posteriormente CS foi sujeita à análise, apoiada em três matrizes orgânicas, na qual foi investigada a linearidade, precisão e limitações da deteção e quantificação. A relação sinal/ruído do sinal derivado da CS foi usada como o parâmetro de quantificação. Para obter uma maior linearidade e precisão, foi acrescentada uma concentração fixa de corticosterona marcada isotopicamente. A seguir, foi detetado claramente o sinal de m/c 347.4 pertencente à CS. A concentração mais baixa da CS extraída do plasma, ainda detetável, foi 0.04 mg/mL, o que apresenta um valor de concentração da CS em sangue de uma tartaruga aproximadamente dez vezes superior ao esperado. Os resultados deste trabalho demonstram que

o método eleito tem potencial de ser utilizado na prática de quantificação de sangue destes animais, embora com algumas limitações.

Palavras-chave: MALDI TOF MS, corticosterona, tartarugas, hormonas de stress, moléculas de baixa massa

Contents

List of Figures

List of Tables

List of Abbreviations

$9-AA$	9-Aminoacridine matrix
ACN	Acetonitrile
$ANOVA$	One way analysis of variance
CDs	Carbon nanodots
$CHCA$	α-Cyano-4-hydroxycinnamic acid
CHO	Cholesterol
CS	Corticosterone
$DESI$	Desorption electrospray ionization
DHB	2,5-dihydroxybenzoic acid
$ECLIA$	Electrochemiluminescence Immunoassay
$EDTA$	Ethylenediaminetetraacetic acid
EIA	Enzyme Immunoassay
$ELISA$	Enzyme-Linked ImmunoSorbent Assay
ESI	Electrospray ionization
FA	Ferulic acid
$Fcrit$	F critical
GR	Graphene
HPA	Hypothalamic-pituitary-adrenal axis
$HPLC$	High-performance liquid chromatography

$IFCN$	Institute for Forestry and Nature Conservation
$ILMs$	Ionic Liquid Matrices
IS	Internal standard
LC	liquid chromatography
LD	Laser desorption
LOD	Limit of detection
LOQ	Limit of quantification
m/z	Mass-to-charge ratio
$MALDI$	Matrix-assisted laser desorption ionization
$MetOH$	Methanol
$MPcs$	Metal-phthalocyanines
MS	Mass spectrometry
MSI	Mass spectrometry imaging
$N-CDs$	N-doped nanocarbon dots
R^2	Coefficient of determination
RIA	Radioimmunoassay
RSD	Relative standard deviation
S/N	Signal-to-noise ratio
SA	Sinapinic acid
$SAMS$	Self-assembled monolayers
SD	Standard deviation
$sDHB$	2,5-dihydroxybenzoic/ 2-hydroxy-5-methoxybenzoic acid
$SIMS$	Secondary ion mass spectrometry
TFA	Trichlorofluoroacteate
TOF	Time-of-flight

Chapter 1

Introduction

Loggerhead sea turtle (*Caretta caretta*) is an omnivorous animal and one of the most abundant and widespread sea turtle species in the Mediterranean Sea [1]. They are capable of travelling hundreds to thousands of kilometers between breeding and foraging areas [2]. North Atlantic loggerhead sea turtles inhabit greatly stochastic environments during their first years of life [3] as the journey, both path and duration, of hatchlings from western Atlantic nesting beaches to eastern Atlantic oceanic foraging areas are determined predominantly at random [4]. Loggerheads pass through the waters around the Azores, Madeira and Canary Islands, an area called Macaronesia [5]. Comparison of loggerheads in 1990 in Azores and Madeira suggested that they migrate in the direction from the Azores to Madeira, as the mean size was found greater for madeiran loggerheads [6]. New technologies, as satellite transmitters, have helped to understand their behavior. Loggerhead turtles are pelagic species in the waters around the Azores and Madeira archipelago [7], they live primarily at the surface as floating and waiting predators during crossing of the Atlantic ocean and in the first years of life [6]. The study of Freitas, Caldeira, and Dellinger researched the surface behavior of ten juvenile loggerhead sea turtles. The turtles were satellite tagged in Madeira island and tracked within 2273 days. This study showed that the amount of time at the surface was greater during the day than night, especially during spring and summer, and as well the time spent at the surface during the day increased with higher air temperatures and weak winds. Turtles tend to dive deeper during clear nights and it may result in increased surface time in order to recover from deeper dives. These findings might be important for conservation of turtles related to operation of anthropogenic activities [8].

Sea turtles naturally encounter a lot of stressors, both anthropogenic and natural [9]. As they are long-lived animals [**Compensatory˙growth˙2003**], the cumulative effect of stressors is high within their life. Another source of

vulnerability to lot of anthropogenic and natural stress is the long duration sea turtles spend in different stages of their life in a diversity of marine habitats: as eggs on the beach, in the open ocean gyres as pelagic juveniles, as as benthic juveniles in nearshore waters, and as adults migrating between feeding and nesting grounds, with different vulnerabilities at each stage [10, 11]. The natural stressors comprise of thermal stress (hypothermia and hyperthermia), seasonal or temperature-related changes in immune function, and the presence of disease, which can be a cause or a symptom of stress. One of the most damaging parasite of loggerhead turtles are spirorchid trematodes, they settle in the vascular system and might affect up to 30% of the west Atlantic loggerhead population [12]. However, the loggerhead turtles in Madeira archipelago have low disease incidence and parasite loads [13]. Natural physiological stressors may be affected or emphasized by anthropogenic factors. For example, physiological responses to natural diving are remarkably different from those caused by the forced submersion of trawl entanglement [14]. Anthropogenic stressors have both direct or indirect impacts on their health. Excessive exposure to the stressors, whether in intensity or duration, leads to dysfunctional debilitating responses [15].

Responses to stress can be at different levels, from the acute stress on catecholamine levels to long term effects, as changes in gene expression, immunological responses (immune suppression), and as well changes in populations, i.g. decrease of reproductive rates [16]. For example, those ones who are exposed to higher stress are more vulnerable to diseases and parasites [17]. Adult sea turtles do not exhibit any avoidance behavior when they find themselves in danger situations, for instance; they very often ingest plastic waste or they encounter an oil slick [18], they as well get entangled in nets or garbage, this is also very common issue in Madeira archipelago. Another threat to sea turtles represents bycatch, discarded and incidental capture of non-target species, by commercial fisheries. Shrimp trawl bycatch of sea turtles has been identified by the National Research Council as one of the most significant source of sea turtle mortality in the United States long time ago (1992) [19]. It was estimated that around 50 000 loggerheads drowned annually due to fisheries in 1980s. As they are very slow to mature, it may take decades to see response in their populations changes [20, 21]. Some of caught turtles are released back to the ocean [22], nevertheless caption triggers stress response [23]. Very common bycatch in Madeira archipelago is caused during black-scabbard fishery when deep drifting pelagic long-lines are used [24, 25]. The foraging oceanic juvenile loggerheads are accidentally caught in drifting long-lines that target blue shark and swordfish as well in Azorean waters [26]. It is estimated that in 2000 as many as 200 000 loggerheads were caught bycatch by the worldwide pelagic long-line fisheries

[27].

Vulnerability to some stressors also differs by ecological niche. For example, polychlorobiphenyl and dichlorodiphenyldichloroethylene accumulations are higher in loggerhead turtle tissues and eggs than in case of green turtles, very likely because of dietary variances [28].

Tourism activities, such as whale watching, jet ski and boat trips, can have negative impacts on wildlife [29], these activities create in Madeira island an additions to income. On the other hand, tourism activities can contribute to the conservation of the sea turtles [30]. It provides information about sea turtles, their ecology and biology, to tourists globally, even those who do not have access to the ocean in their own country [31]. In the study of Tisdell and Wilson, the majority of respondents (87%) said that after their experience of sea turtles tourism they would take more personal action to conserve sea turtles and 98% of respondents think that more action should be taken to minimize threats to marine turtles [32]. In Madeira island was issued the first Portuguese law to protect sea turtles in September 7Th, 1985 [33]. The legislation to regulate the pelagic vertebrate observation tourism industry, commonly know as whale-watching boats, was issued 14Th of May 2013. There were applied rules that are supposed to prevent perturbation of marine animals within observation and approximation of boats. It is necessary to avoid the production of the noise that may disturb or attract them. During any kind of operation it is prohibited: Persecution of marine vertebrates, which is considered to be any attempt to approach or accompany them which leads to escape or disturbance behavior; Cause the separation of the group, especially the isolation of juveniles; Use techniques to attract marine vertebrates which, according to scientific evidence, have a negative impact on both marine vertebrates and ecosystems; Touching marine vertebrates. The exception is if the animals are entangled in garbage and one touches them with the intention of helping them; Throw any objects at the turtles; Enter the water to intentionally interact with sea turtles; Nocturnal observations of vertebrates; Approach closer than 25 metres from a turtle within observation and 50 metres within sailing; Exceeding a speed of 8 knots between 100 and 50 m from the animals; Staying longer than 10 minutes in the area of observation; If the animal shows sings of disturbance behavior, the water-crafts must sail away [34]. With intensive boat trafficking the basking of turtles is threatened, they do not bask as deeply when many boats, mainly sport fishermen, sail the waters. Therefore it is necessary to evaluate the stress of wild-turtles to determine the effects of whale-watching and boating. Besides, this technique is also helpful when following the turtles during rehabilitation which may last many months.

Loggerhead sea turtle can serve as effective bioindicator of marine ecosys-

tem health, due to its molecular stress responses, and can be used as a monitor for pollution [35]. In most parts of the world are protected, as well as in Madeira archipelago [33, 36].

1.1 Determination of Stress Hormones

Increase of of the adrenocortical steroid corticosterone due to stress has been demonstrated in a variety of reptiles. The hypothalamic-pituitary-adrenal (HPA) axis of wild and immature loggerhead turtles is sensitive to stress and it can be observed by increase of plasma corticosterone concentrations [37], causing changes in the leukocyte components, circulating lymphocytes adhere to the walls of blood vessels, and afterwards are subjected to transmigration from circulation into other tissues (lymph nodes, spleen, bone marrow and skin). This exodus causes a significant reduction in their circulating numbers. On the contrary, glucocorticoids also stimulate an influx of neutrophils into the blood from bone marrow and reduce the efflux of neutrophils from the blood to other compartments. One possible approach to measure turtle's stress is to run a blood test and observe the representation of different cell types. However, the most reliable method to evaluate the physiological stress is the measurement of glucocorticoid hormones levels in plasma [9]. The levels of corticosterone present in plasma differ within size of turtles, smaller turtles exhibit lower values, and also by season, lower values of corticosterone were observed in winter season, it might be caused by temperature and reproduction conditions. In most of the species, the levels of corticosterone are stable during the first three minutes after capture/ stress factor. The highest concentrations occur three hours after capture/stress factor. The study of Gregory et al. the initial levels of corticosterone were between 2.3 to 10.3 ng/mL. Three hours after capture the concentrations increased up to 25.15 ng/mL. However, mean initial corticosterone concentrations of turtles captured by tangle net are among the lowest values reported for reptiles, between non-detectable level under 0.05 to 11.85 ng/mL [38]. Differences in concentrations of corticosterone among individuals provide information about physiological conditions [35]. Figure 1.1 shows levels of plasma corticosterone during captivity of small loggerhead turtles depending on the time and method of capture [38].

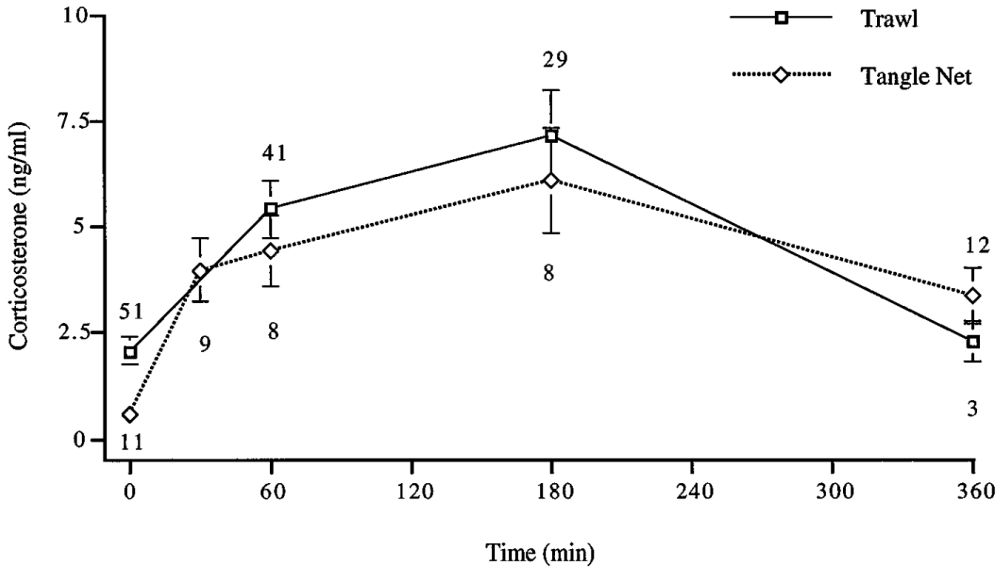

Figure 1.1: Mean plasma corticosterone levels (ng/mL) over time for small loggerhead turtles (Caretta caretta) captured by trawl or tangle net. Numbers by means (±SE) indicate sizes of turtles. Adapted from Gregory et al. [38].

There exists many approaches how to asses corticosterone levels in plasma. The most common ones are an Enzyme Immunoassay (EIA), Enzyme-Linked ImmunoSorbent Assay (ELISA), radioimmunoassay (RIA), electrochemiluminescence immunoassay (ECLIA), high-performance liquid chromatography (HPLC) coupled to electrospray ionization mass spectrometry (ESI-MS) [39, 40, 41, 42]. Despite the efficiency, these methods might not be accessible at every institution. The enzyme-based quantification has low reproducibility, radioactivity-based measurements are time consuming and performed under strenuous guidelines for radioactivity precautions. Another drawback is the accuracy of all the immunological quantification assays which is suboptimal due to the imprecision of antibody recognition [43]. The matrix-assisted laser desorption ionization time-of-flight mass spectrometry (MALDI-TOF MS) is widely used technique for analysis of biomolecules (such as peptides, protein and saccharides) and large organic molecules (polymers, dedrimers etc.) [44]. However, nowadays this method is used also for the detection of low molecular weight substances [44, 45].

1.2 Principles of MALDI Mass Spectrometry

MALDI is an accurate, rapid and cost-effective method. It has been extensively used since the late 1980s, especially in the analysis of large molecules [46]. The capability of MALDI to rapidly characterize microorganisms and large molecules promotes its potential applications in many areas, such are bio-defense, environmental monitoring, medical diagnostics, and food quality control [47]. MALDI-TOF MS is used in many clinical laboratories for various applications. Latter reports show that MALDI can be also used for quantitative determinations of drugs in tissues by implementing internal standard [48].

A mass spectrometer consists of three functional units: (1) an ion source which ionize and transfer sample ions into a gas phase, (2) a mass analyzer that separates ions based on their mass-to-charge ratio (m/z), (3) a detection device that records separated ions. Laser desorption (LD) was coupled to several kinds of mass analysers, such as time-of-flight [49]. TOF mass analysers are convenient for interfacing with pulse laser ionization and offer the possibility of rapid analysis and miniaturization [50]. In MALDI analysis, a sample is mixed with a matrix on a conductive metal plate, which results in the crystallization of the sample within the matrix and formation of, so called matrix/analyte co-crystals. Many factors can affect the quality of obtained spectra, but the application of sample on the MALDI target and the matrix selection, play a crucial role. There are many types of application approaches of sample on the plate. After the crystallization of the sample and matrix, the plate is introduced in the mass spectrometer and it is bombarded with short laser pulses. Laser emits the light usually in the UV or IR range. The matrix absorbs energy from the laser, it leads to the desorption of the analytes which are later on vaporized and ionized. Matrix assisted desorption and ionization process of the analytes results in the formation of ions carrying different charges, the position of which is indicated as the mass over charge ratio (m/z). Although no general rule can be established and the number of charges depends on the nature of the sample, it seems that mostly a singly positively - or negatively-charged ions are generated during this process. Desorbed ions are accelerated through an electrostatic field and then they are ejected through a metal flight tube which is subjected to a vacuum till they reach a detector. This is, so called, "field-free time-of-flight" mass analyzer, reached by the ions with same kinetic energy. Afterwards, smaller ions travel faster than larger ones.

MALDI positive ion mode ionization process includes two main steps: (1) the excitation and self-ionization of matrix compound upon absorption of the laser energy with a specific wavelength to create protonated matrix molecules,

and (2) transfer of gas phase proton from the protonated matrix to more basic analyte molecules to produce the protonated analyte for MS detection. Upon the presence of other inorganic cations, such as Na^+ or K^+, also Na^- or K^- adducts can be formed. Negative ions are produced when the deprotonated matrix abstracts a proton from the analyte compound [47]. Bioanalytes with different m/z which formed a complex sample are separated pursuant to their TOF and create a mass spectrum. Mass spectrum is described by the m/z and the intensity of the ions, m/z corresponds to the time when the ion reaches the detector, the time is then converted to m/z. The intensity represents the number of ions. Simplified technical description of MALDI-TOF MS is described in Figure 1.2.

1.3 Advantages and Disadvantages of MALDI

The advantages of MALDI MS are:

1. it creates uncomplicated mass spectra, since mostly singly-positively/negatively charged ions are detectable in the spectra.
2. it has high throughput (fast spectra acquisition) ,
3. wide application range (various types of analytes and a wide mass range, up to 300 kDa),
4. low sample consumption,
5. ease of use,
6. it is inherently robust [51].
7. No derivatization or purification of samples are necessary in MALDI methodology [45].
8. MALDI approach eliminates contamination during the process of analysis of environmental and biological samples [52].
9. MALDI can be automated or semi-automated system, which represents an advantage for analysis with large amount of samples or analysis that take lot of time.
10. It exhibits very high accuracy compared to other techniques, in study Savas et al. [53] MALDI TOF identified 30 urinary isolates with 100% accuracy.

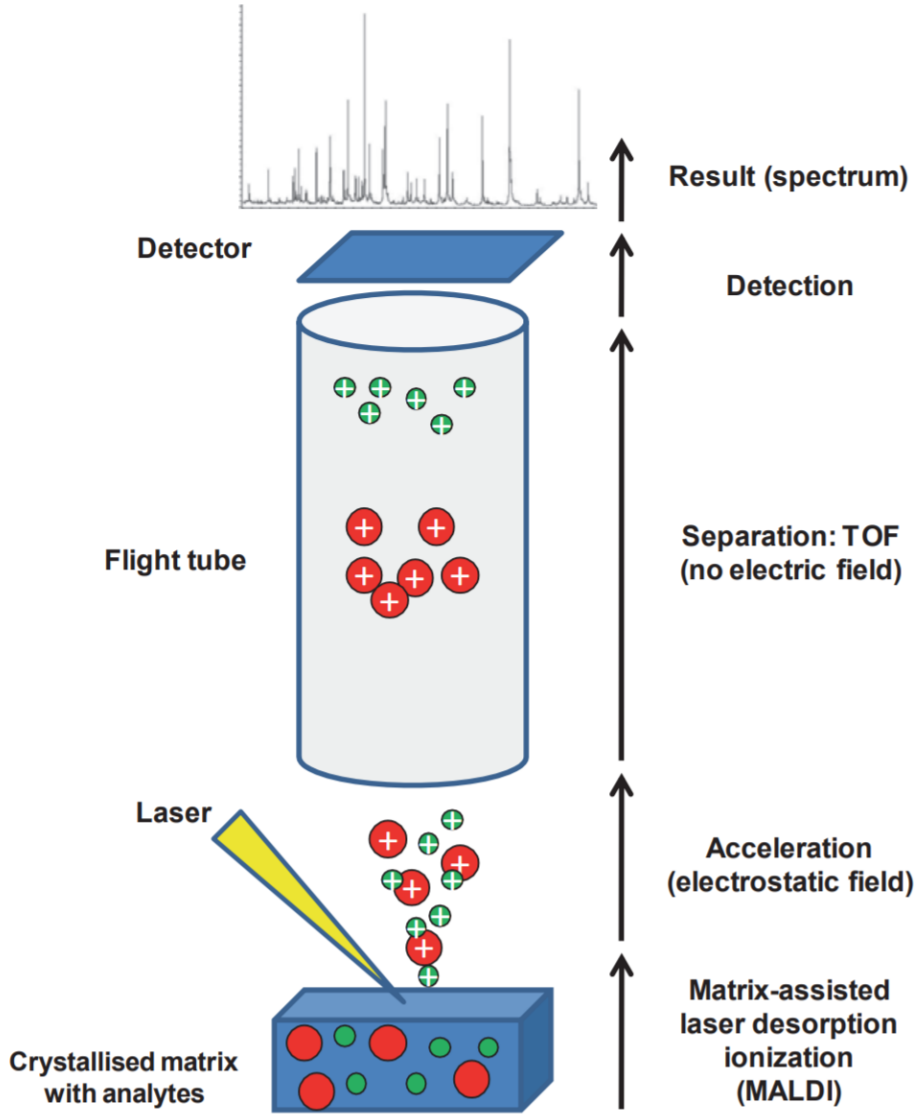

Figure 1.2: Technical description of MALDI-TOF MS. First, the sample is mixed with a matrix on a conductive metal plate and dried. Second, the metal plate is introduced in the mass spectrometer and is bombarded with brief laser pulses. Third, the desorbed and ionized molecules are accelerated through an electrostatic field and then ejected through a metal flight tube exposed to vacuum until they reach a detector. Bioanalytes are separated according to their TOF, smaller ions fly faster than larger ions. Mass spectrum is created by mass to charge ratio (m/z) peaks with varying intensities [50].

Analysis of complex sample matrices such as serum or plasma might be problem for MALDI technique due to ion suppression of analyte. However, it has been shown that use of suitable sample preparation protocols, similar to those applied in LC-MS(/MS) methods, eliminates components causing co-crystallization issues and induces ion suppression [45]. Although MALDI has good performance in analysis of high-molecular-weight molecules, it shows drawbacks in analysis of low mass molecules due to the interference from background matrix below m/z 600 [46].

1.4 Detection of Small Molecules by MALDI

As was mentioned before, MALDI has limitations in analysis of small molecules due to the background interference from commonly used MALDI matrices which can overlap with characteristic ions of analyte and caused ion suppression in MALDI spectrum [51]. However, one of the possibilities how to overcome this problem is development of suitable method, specific sample preparation such as analyte/matrix derivatization, selection of propriate matrix, addition of dopants and adequate deposition technique [54]. There have been designed different materials, for example magnetic nanoparticles, porous silicon or TiO_2, in order to immobilize classic matrix [55]. The matrix effect can be also repressed if the analyte is significantly more basic than the matrix [47]. To keep the advantages of MALDI, such as fast analysis and no need for sample and matrix derivatization, or separation, scientists are more focused to find the appropriate matrix, sample application technique and instrumental parameters to overcome the low detectability of small molecules.

One of the options is use of seed-layer surface preparation method when homogeneous matrix layer is first formed by deposition of the matrix dissolved in a volatile solution onto the MALDI sample, followed by facilitated evaporation of the solvent. After a formation of a thin matrix layer, the matrix/sample mixture is applied to the pre-deposited matrix spot for MALDI MS analysis. In the study Ho et al. [51], seed-layer method enhanced MALDI MS detection and demonstrated higher sensitivity, resolution and reproducibility compared to the conventional methods. However, seed-layer preparation of small molecules with different polarities needs further optimization.

The use of self-assembled monolayers (SAMS) of alkane thiolates on gold with subsequent detection on MALDI and the use of a pyrene moiety tag to promote ionization without a matrix was also reported in the literature. Neverthless, these methods are not suitable for routine and fast analysis because of the lack of availability of SAMS plates and the unavoidable product

modification in the pyrene tag method [47].

In terms of potential quantification, internal standards (IS) that are structurally similar to the analyte can be used to partly conquer variation caused by inhomogeneity of the sample/matrix co-crystals distribution on the plate. The analyte and IS should be with similar mass and ionization properties. It might be difficult to find suitable internal standard. Use of IS still can cause unpredictable discrimination effects in sample matrix co-crystallization or ion suppression in the desorption ionization process [51].

Decision tree (Figure 1.3) might help to decide if MALDI is an appropriate analytical method for detection of low mass molecules.

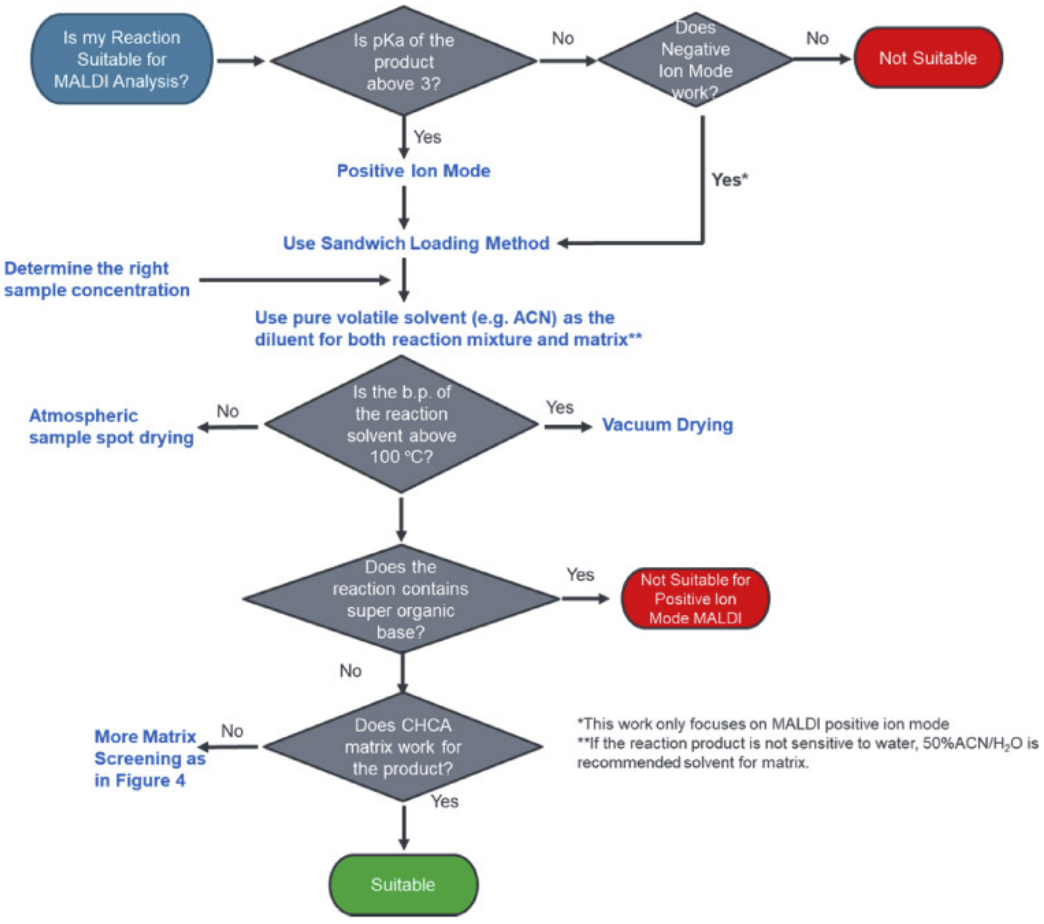

Figure 1.3: Decision tree for selection of MALDI MS as an appropriate analytical method for determining small molecule reaction mixture [47].

The matrix composition differs according to the molecules to be analysed and the type of laser used. Usually, matrix is composed of small acid molecules that have a strong optical absorption in the range the laser wavelength used. The most commonly used matrices are: 2,5-dihydroxybenzoic acid (DHB), α-Cyano-4-hydroxycinnamic acid (CHCA), sinapinic acid (SA), ferulic acid (FA), 2,5-dihydroxybenzoic/ 2-hydroxy-5-methoxybenzoic acid (sDHB) or 9-Aminoacridine matrix (9-AA). Each of them is suitable for different types of analysis. While DHB shows the best application for the detection of glycopeptides and glycoproteins, FA, SA, and CHCA appear to be efficient for the detection of protein biomarkers. DHB and CHCA are convenient for the detection of lower weight molecules if the correct solvent is used, whereas SA and FA are better for the detection of higher mass molecules. CHCA seems to be suitable for both [50]. CHCA also enables highly sensitive measurement of peptides and proteins from 0.7 to 20 kDa [56]. DHB was shown as a suitable matrix for the analysis of cholesterol [57]. SDHB is eligible for the generation of In-Source Decay spectra of intact proteins or analysis of very large proteins and glycoproteins [56]. The pKa of CHCA and DHB are 1.17 and 2.95, respectively. Therefore these matrix molecules are able to transfer a proton to more basic molecules during positive ionization process [47].

Metal-phthalocyanines (MPcs) can also be used as MALDI matrix for detection of small molecules [58]. Another option is use of Ionic Liquid Matrices (ILMs), protic ionic liquids synthesized by mixing conventional acidic MALDI matrices with an equimolar number of organic amines, which have been introduced almost 20 years ago as alternatives to crystal matrices. Their capability to reduce the background on mass spectra and possibility of the quantitative analysis of small molecules is the reason why they are suitable matrix for low mass molecules. It was shown their application improve relative standard deviations, or has similar precision compared to conventional matrices, and also the application of ionic matrices based on DHB and CHCA acids, shows advantages for some of the quantification of small molecules compared to conventional matrices. However, on the other way the lower potential of ionization and fragmentation of molecules with ILMs requires higher laser energy in order to obtain any spectrum compared to conventional matrices [59].

Another option is so called reactive matrix which can enable analysis of small molecules by increasing their final m/z value or lowering their volatility [54]. Normally, before the analysis, the resulting derivatives are subjected to traditional sample preparation for MALDI mass spectrometry by mixing with a matrix. In the work of Zhang and Gross was introduced new principle which use compounds for derivatization that exhibits dualistic properties,

concurrently behave as derivatization agents and as matrices providing high desorption/ionization efficiency [60]. The development of reactive matrices approach focused on the selection of compounds optimally convenient for the derivatization of carbonyl compounds, especially, hydrazides and substituted hydrazines [61].

1.5 Nanoparticles in MALDI Analyses

As it is difficult to measure small molecules with MALDI TOF MS [62], nanomaterials have been developed and tested as assisted matrices/ substrates of laser desorption/ionization (LDI) examining small molecules. Wide range of nanomaterials have been applied in MALDI analysis, such as: nanopost arrays, silicon materials (e.g., silicon nanowires, nanoporous silica) [63], gold film, titanium dioxide nanoparticles [64], germanium nanodots, structured aluminum foil, silver nanoparticles, [51] carbon materials (e.g., graphite, carbon nanotubes, fullerene, graphene, or carbon nanodots) [46]. Due to their large surface area-to-volume ratio, addition of nanomaterials provides a lower number of signals with lower intensity mass spectrum in the low mass regions (< 500 Da) [51], they also act as laser absorption matrices to provide efficient ionization in the MALDI-TOF MS analysis of small molecules [64] and enhance the sensitivity of the LDI MS analysis of complex samples [52] as the competition of analytes and matrix is eliminated in the process of ionization [52]. Use of carbon nanodots (CDs) has excellent shot-to-shot reproducibility because there is possibility to avoid the co-crystallization process that usually produces an inhomogeneous composition and results in "hot spots" when using traditional matrices, it is due to its excellent water-solubility [46]. In addition, CDs were shown to be able to overcome the cholesterol-derived ion suppression in the presence of high content of inorganic salts [65].

1.6 MALDI and Other Techniques

Mass spectrometry imaging (MSI) is an useful analytical tool that provides complementing information to that obtained through other analytical techniques and imaging methods. Compared to other clinical diagnosis methods, such as electrochemical immunoassay, flow cytometry, ELISA etc., MALDI-TOF MS shows better sensitivity and specificity and allow to observe directly molecular weight specific peaks to demonstrate the presence of target biomarkers [63].

MALDI, desorption electrospray ionization (DESI) and secondary ion

mass spectrometry (SIMS) are ionization methods frequently used in MSI [48]. As MALDI and SIMS are initiated by fast energy deposition events in the surface region both techniques might seem similar. In SIMS a high energy primary particle hits the surface and initiates a collision cascade that leads to uplifting of intact molecules from surface. The physics of the collision cascade does not require that the atoms move together. The physics of ablation demands that a large amount of material move in a concerted fashion towards the vacuum. In MALDI, matrix/analyte co-crystals are irradiated by laser and then the large analyte-derived are desorbed from the surface intact. The difference between SIMS and MALDI techniques is in the size of the ions that are detected. The upper mass limit for organic molecules in SIMS is in the range of 10–12 kDa, whereas for MALDI it is $\sim$ 1 MDa [66, 67].

MALDI and electrospray ionization (ESI) are both soft ionization methods that allow ionization and vaporization of large non-volatile synthetic and biological macromolecules, such as an intact proteins. ESI generates multiply charged ions which complicate interpretation and frequently abducts with organic solvents are generated, while MALDI produces mostly singly charged ions, therefore MALDI spectra can include larger numbers of proteins [50, 49].

MALDI and liquid chromatographic (LC) methods can be both applied for some sample analysis, with the difference that MALDI does not involve a mobile phase and has some advantages over LC-MS, such as easier sample preparation, simple analysis procedures, and lower instrumentation costs [68, 69].

MALDI-MS could be considered as an effective alternative to ESI-MS in the electrochemical measurements, whereas MALDI is less affected by salts and buffers which are often used as supporting electrolytes [70]. In LC-MS after repeated sample injection occur strong signal suppression and carry-over issues due to the high basicity and relatively non-volatile character of many organic reactions [71, 72]. LC-MS analysis are vulnerable towards cross contamination as the reaction mixture is in direct contact with ESI source. Frequent wash and maintenance are necessary for LC-MS due to preventing contamination and clogging of the column and ESI capillary. Another differences towards LC-MS are ability to rapidly test multiple reaction products simultaneously, and high robustness towards base and catalyst interferences on detection signals [47].

1.7 Aim of the Study

The aim of this study is to develop an effective and working method of corticosterone detection by MALDI-TOF MS, which can be applied for evaluation of turtle's stress and help with understanding of their jeopardy and protection. There exist another studies dealing with detection of small molecules by MALDI-TOF MS [73, 58, 74, 75], however there are not many studies about corticosterone detection by MALDI-TOF MS, especially with simple workflow available to all laboratories with limited equipment and resources.

The process is subdivided into the following goals:

- To select suitable organic matrix using cholesterol as a model system.
- To test the applicability of nanomaterials (carbon dots, N-doped carbon dots and graphene) as an approach to overcome potential cholesterol-arising signal suppression by matrix signals in the presence of increasing concentrations of NaCl, as salts are part of physiological solution.
- To test the detectability and potential for quantification of corticosterone by MALDI TOF MS.
- Finally, to check the detectability of CS in a blood of *Caretta caretta* and all related procedures as extraction of corticosterone from turtle's plasma and detection limit determination.

Figure 1.4: Loggerhead turtle, *Caretta caretta*.

Chapter 2

Materials and methods

2.1 Materials and Chemicals

Internal standard (IS) Corticosterone-9,11,12,12-d_4 98 atom % D, 97% (CP) with molecular weight 350.49 and Corticosterone powder $\geq$ 98.5% (HPLC) with molecular weight 346.46 were obtained from Sigma-Aldrich (Germany). Cholesterol powder $\geq$ 99% with molecular weight 386.65 was obtained from Merck (France) and acetonitrile for LC-MS from POCH S.A. (Poland). Concentration of stock solution was 1 mg/ 10 mL. Methanol was obtained from CHEM-LAB (Belgium). Matrices for MALDI TOF MS (2,5-dihydroxybenzoic, 2-hydroxy-5-methoxybenzoic acid (sDHB) and also 2,5-dihydroxybenzoic acid (DHB)) were acquired from Tokyo Chemical Industry (Tokyo, Japan) and prepared in methanol at concentration 10 mg/mL. α-Cyano-4-hydroxycinnamic acid (CHCA) was purchased from Sigma Aldrich (Germany). Ethylenediaminetetraacetic acid (EDTA) was obtained from Sigma-Aldrich (Germany) and dissolved in water (final concentration 1mg/mL). Blood samples were taken into VACUETTE NH Sodium Heparin 4 mL Greiner Bio-One (Germany). Diethyl Ether stabilized with $\sim$ 6 ppm of BHT was obtained from PanReac AppliChem ITW Reagents (Spain).

2.1.1 Synthesis of Carbon Dots Nanoparticles

Carbon dots were prepared by Dr. Manuel Algarra at Department of Inorganic Chemistry, University of Malaga, Malaga, Spain. Briefly, they were prepared by a hydrothermal approach from lactose [76]. Shortly, lactose was treated in a Teflon lined steel reactor with HCl (1 M) at 100 ℃for 3 hours in an oven. Hereafter, the mixture was dialyzed against deionized water for 24 hours. N-doped CDs (N-CDs) were prepared by mixing CDs with 1,6-hexanediamine (1 g, 98%, Sigma-Aldrich, Germany) in a Teflon lined steel

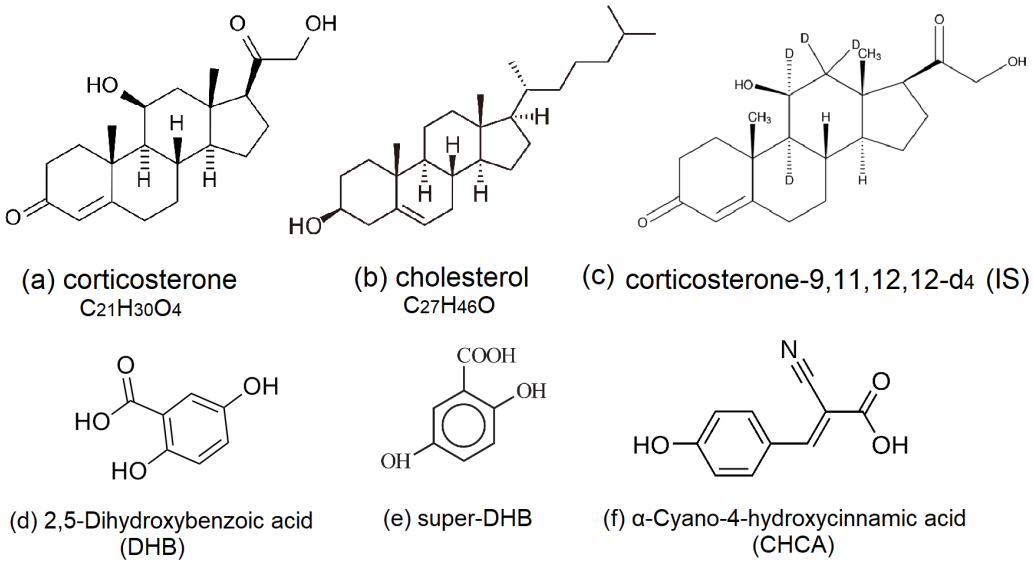

Figure 2.1: Chemical structure of (a) corticosterone, (b) cholesterol, (c) IS, (d) DHB, (e) sDHB, (f) CHCA and (g) N-CDS.

reactor, and heated in an oven for 3 hours at 100 ℃as described in Figure 2.2. The maximum particle height was 21 nm and 13 nm for the 25 μm^2 and 6.25 μm^2, respectively, displayed by 3D topographic images obtained by AFM. Diameter of nanoparticles was calculated by a circle approximation, it was found 165 particles with a diameter between 0 and 50 nm, 39 particles with a size range between 50 and 100 nm, and 15 particles with sizes above 100 nm, N-CDs particles had dimensions in a nanometer range, with a spherical shape distribution. The shape of CDs was a well dispersed, spherical and not aggregated with a mean value of 7.8 nm [65].

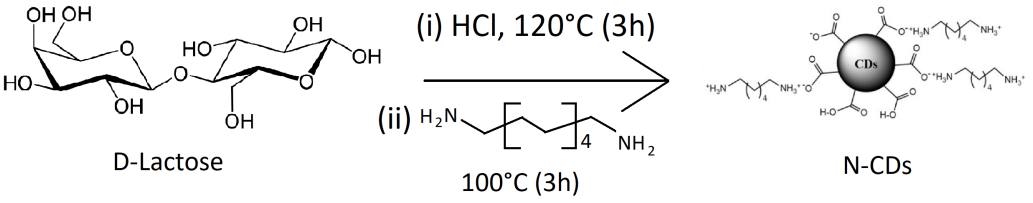

Figure 2.2: Molecular representation of obtained N-CDs.

2.2 Turtles Capture Method and Sampling Procedure

Loggerhead turtle (*Caretta caretta*) was captured 3rd of July 2020 by rescue workers nearby Cais de Areia, Porto Novo, in Atlantic ocean in Madeira Autonomous Region. It was given her ID 1907. The turtle was found in bad conditions with a spine deformity, floating on the surface, consequently she was transported to Marine Biology Station of Funchal in Lido where the turtle received antibiotic treatment and was kept in tanks till recovery. The turtle weighted 11650 g at arrival and was very emaciated. The curved carapace length was 545 mm. Approximately 3 mL of blood was taken from the dorsal post-occipital sinus 13th of July 2020 at 11:30. Blood collection was repeated 5th of November 2020 at 15:30 after recovery of the turtle when she weighed 15060 g. Blood was stored in test tube containing EDTA and Vacuette test tube containing sodium heparin as preanalytical solution. Samples were immediately transported to CQM laboratories and centrifuged with 2 500 rpm for 15 minutes. Plasma was removed and stored in freezer in -26 ℃ until conducted analysis. The turtle was released 7th of November 2020 back to the ocean.

Figure 2.3: Loggerhead turtle (*Caretta caretta*), ID 1907.

2.3 Ethical Statement

Trapping and captivity of loggerhead turtle was approved by Institute for Forestry and Nature Conservation (IFCN) of Madeira Autonomous Region. The license N°03/IFCN/2020–FAU MAD is enclosed in appendix as Figure 4.1 and 4.2. The turtle was treated carefully and blood samples were taken by a licensed veterinarian.

2.4 Extraction of Corticosterone from Plasma

Corticosterone was extracted from plasma by using an ethyl ether. Sample of plasma was mixed with ethyl ether in ration 1:10, respectively, then vortex for 3 minutes and centrifuged for 3 minutes at 2500 rpm allow the phases to separate. The organic phase was transfered into a clean tube and the solvent was evaporated with a stream of nitrogen gas. The residue was dissolved in 10 μL of ACN/MetOH and vigorously vortexed. Samples with addition of 10 mg/mL IS were included to extraction procedure as a control.

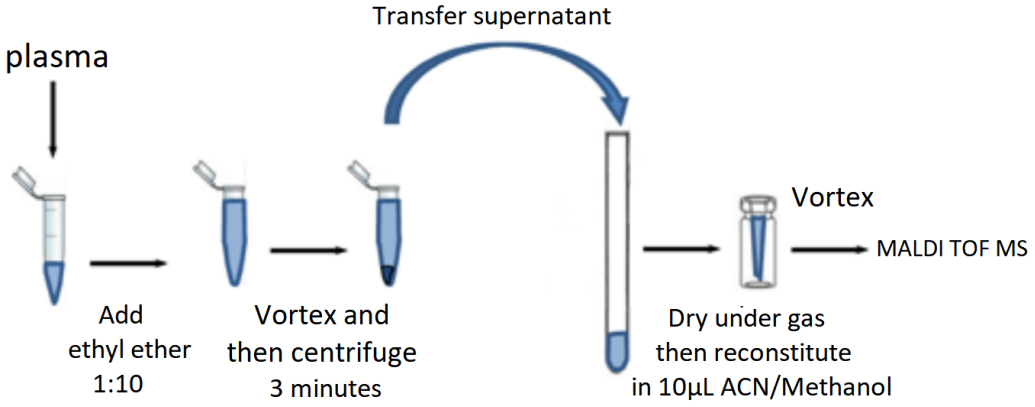

Figure 2.4: Corticosterone plasma extraction procedure.

2.5 MALDI TOF MS

2.5.1 Instrumental Parameters

MALDI TOF mass spectrometry was performed using the Bruker Autoflex maX Matrix-Assisted Laser Desorption and Ionization (Time-of-Flight) 2 Mass Spectrometer MALDI TOF/TOF MS with proprietary smartbeam-II™

laser technology and high dymanic range FlashDetector™ system in conjuction with a 10 bit 5 Gs/s digitizer and PAN™ wide mass range. The TOF mass analyzer was operated in the positive-ion mode at a laser frequency of 200 Hz in a mass range 300 - 680 Da. The acceleration voltage was set to 20 kV, and the time of extraction delay was 120 ns. Detector was checked before conducted sampling, method and spectra were calibrated by setting the signals arising from DHB to their precise value (m/z). Each spectrum corresponds to the ions obtained from 2000 laser shots fired on the ground steel/ AnchorChip MALDI target plate and acquired using the Flex Control v.3.4 software (Bruker Daltonics). The laser intensity was set up at 30% for CHCA, 50% for sDHB and 60% for DHB samples. The spectra were visualized and data processed using Flex analysis v.3.4 software (Bruker Daltonics).

2.5.2 Application of Samples on MALDI Target

The MALDI plate was spotted using the sample-first technique and the dried-droplet technique in case of cholesterol analysis. In case of corticosterone analysis was applied the dried-droplet technique and sandwich method. The sample first technique consist in applying 1 μL of the sample on the plate when the sample is dry it is overlaid by 1 μL matrix. The dried-droplet technique is prepared as a pre-mix. Equal volume (2 μL) of sample and matrix were placed into Eppendorf tubes and vortex. Then, 0.5 μL of the mixture solution was deposited in quadruplicate into the wells on a stainless steel target plate. In the case of the sandwich method, 0.5 μL of the analyte is applied first, and only when the analyte dries, it is overlaid by 0.5 μL of a matrix. There exist many types of plate drying approaches. Atmospheric pressure approach was used for sample/matrix co-crystallization. It is one of the slowest method, however this method gives the most uniform and best centered dried spot MALDI plate as suggests study of Blincoe et al. [47]. For cholesterol analysis ground steel target plate was used. For corticosterone analysis was chosen AnchorChip target plate which contains anchors, hydrophilic patches surrounded by a hydrophobic ring. The anchor restrains droplets at the sample position and the hydrophobic ring prevents spreading of sample and concentrates the sample into a spot 800 µm in diameter [56].

Figure 2.5: AnchorChip stainless steel MALDI target plate used for corticosterone assay.

2.5.3 MALDI Maintenance

Poor cleaning of the MALDI plate between runs and inappropriate deposit of the sample on the plate may cause affection of results. To avoid this the MALDI plate must be properly maintained. Bruker suggests to use trichlorofluoroacteate (TFA) or guanidium to clean microplates between applications. However, as TFA exhibits occupational hazard (eye, skin, and respiratory toxicity), there was used an alternative protocol, proposed by Bruker, to clean stainless steel MALDI TOF plate. Plate was mechanically cleaned by H_20 and methanol, placed to the box with isopropanol and left 10 minutes at ultrasound treatment.

Results might be also disturbed by technical problems and/or poor maintenance of the MALDI TOF instrument. The presence of dust on plastic joints or the aging of these plastic joints can lead to vacuum failure and cause functional disturbance. MALDI TOF MS should be placed in clean area without drafts to avoid dust exposure. Uncleanliness of laser source could cause other problems, the level of impurity present on the laser source may be indirectly measured according to the number of shots needed to acquire a correct identification [50, 56]. Maintenance of MALDI TOF device was done regularly and according all the instructions of Bruker.

2.5.4 Analysis of Cholesterol by MALDI-TOF MS

It is known that matrix-solvent composition and sample preparation are important factors that influence the quality of MALDI mass spectra [57]. The key factors identified through method development were matrix selection, matrix/analyte spotting mechanism, sample dilution and concentrations, plasma extraction, and consideration of other reaction components. For quantitative or semi-quantitative analysis of reaction mixture, the MALDI sample concentration should be first diluted and optimized to prevent the detector saturation by intense MS signals [47].

Cholesterol was used as the model system for the development of the method for quantification of corticosterone levels in blood of turtles, because MALDI is not used as the routine method for quantification. The following parameters were tested: the concentration dependence, procedure for application on the MALDI target (dried-droplet and the sample first technique), and the presence/concentration of carbon-based nanoparticles on the sample plate. The effect of NaCl was evaluated to check the detectability of cholesterol in physiological solution. Cholesterol solutions were prepared by dissolving a precisely-weighed quantity of cholesterol (M = 386.67 g/mol) in acetonitrile. Cholesterol powder was dissolved in acetonitrile to a molar concentration 25.9 μmol/L. Thereafter different matrices were tested with variation of concentrations of cholesterol in range 1 μg - 0.75 ng to find the most suitable conditions for detection. (I.e. the concentration range in which the response of the CHCA, saturated CHCA (NPs), DHB, sDHB, carbon dots (CDs), graphene (GR) and N-doped carbon dots (N-CDs) were used.) Matrices and cholesterol solution were applied on the plate by two approaches: (I) "dried-droplet method", i.e. matrix and cholesterol solution were mixed before application on the plate in ration 1:1. (II) "the sample first technique", cholesterol solution was applied first, and the same volume of matrix/NPs solution applied over. Mixture was left to dry at the room temperature. Ground steel plate was inserted into MALDI TOF device, spectra acquired and processed by using Flex Analyses v.3.4 software. Values of signal to noise ration of the signal at m/z 369.3 arising from cholesterol were recorded, statistically processed and compared to find the best condition for quantification.

2.5.5 Detection of Corticosterone by MALDI-TOF MS

Powder of 98.5% corticosterone was dissolved in acetonitrile and methanol to a concentration 28.9 μmol/L as a stock solution. For the diluent, solution of ACN and methanol was used in ration 1:1 (v:v). ACN is the preferred diluent

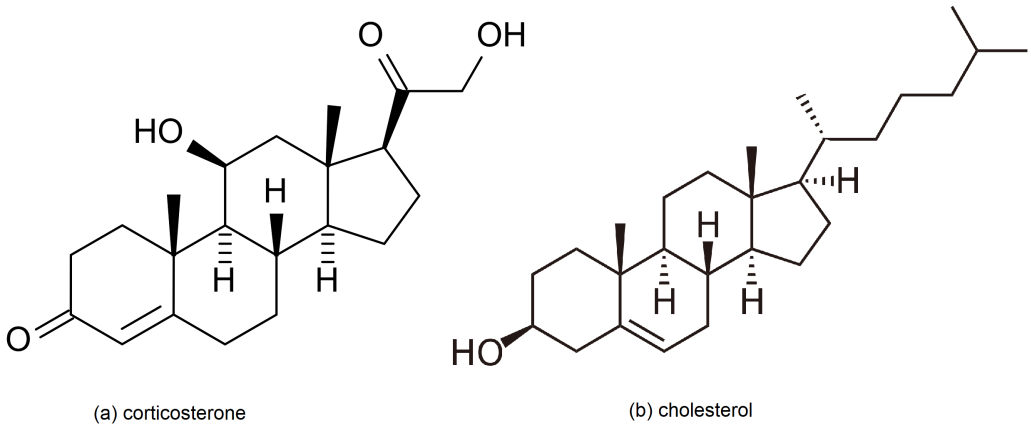

Figure 2.6: Chemical structure of (a) corticosterone, molar mass 346.5 g/mol, and (b) cholesterol, molar mass 386,654 g/mol.

since it forms better droplet on the stainless steel MALDI plate, methanol has poor adhesion on MALDI plate, however ACN could not be used alone due to the low solubility of CS in ACN. From stock solution were prepared concentrations of CS in range from 5 mg/mL to 0.61 mg/mL. As a quantitation approach for reaction profiling using MALDI-MS was chosen absolute quantitation using an isotopic labeled internal standard. This approach is more suitable for reaction optimization in analysis where there is a single product across the whole MALDI plate [47]. Internal standard of corticosterone was dissolved in solution of ACN/MetOH to a concentration 10 mg/mL. Afterwards solutions of CS with internal standard were prepared, CS was mixed with 2.5 μL IS 10 mg/mL to final volume of 200 μL and 62.5 μL. Concentration range from 5 mg/mL to 0.16 mg/mL of CS, total of six concentrations, was prepared and analysed. Three different matrices were tested: CHCA, sDHB and DHB all in a concentration of 10 mg/mL. All samples mentioned above were applied on MALDI anchor chip plate in quadruplicate, that was chosen due to better adhesion of the samples to the plate, by dried-droplet technique as described in section 2.5.2. Analysis were repeated three times in different days in order to obtain statistical significance and day-to-day reproducibility. Spectra was acquired and processed by using Flex Analyses v.3.4 software. Signals were observed and different conditions of sample preparation were compared. Values of signal to noise ration of the signal at m/z 347.4 arising from CS were recorded and statistically processed.

2.5.6 Preparation and Detection of Plasma Samples for MALDI-TOF MS

Corticosterone was extracted from plasma as it is described above in section 2.4 and analysed by MALDI-TOF MS. Afterwards, each plasma sample was spiked with 10 μg/mL CS and ACN/MetOH mixture was added to obtain final concentrations of CS from 5 mg/mL to 39 μg/mL and then plasma was extracted following extraction procedure. Another set of samples were spiked with 10 μg/mL labeled IS till final concentrations of CS from 5 mg/mL to 39 μg/mL. Thereafter the samples were subjected to MALDI-TOF MS analysis. Samples were prepared in quadruplicate, MALDI mass spectra were acquired with CHCA, DHB and sDHB matrices and repeated three times in different days. MALDI spectra were acquired and processed by using Flex Analyses v.3.4 software. Signals and S/N ratio values at m/z 347.4 and 351.4 were detected, recorded and statistically processed.

Figure 2.7: The MALDI TOF/TOF MS (Bruker Autoflex maX) equipment installed in CQM.

Chapter 3

Results and discussion

3.1 Overview

In this work, the conditions to analyze small molecules, id est stress hormones in blood of sea turtles by MALDI TOF MS was investigated. In the first part, cholesterol was used as a model system because it is a highly studied biological compound due to its structural importance in lipid membranes and the damaging effects caused by its oxidation [57]. Both, cholesterol and corticosterone, have a steroid character, and similar molar mass, i.e. 386.6 g/mol for cholesterol and 346.5 g/mol for corticosterone. The first step of the work was to choose ideal matrix for cholesterol/ corticosterone detection.

3.2 Quantification of Small Molecules with Cholesterol as a Model System

The signal at m/z 369.3 emerges from dehydrated cholesterol, followed by the addition of a proton (M-H_2O+H), that is easily detectable species of cholesterol in the MALDI TOF mass spectra. Other observable signals arise from oxidation products of cholesterol, they are results of the process which can occur upon laser illumination [57]. One of these signals is at m/z 381.2 and often surpass signal at m/z 369.3. Because cholesterol has a rather poor ion yield, higher initial solution concentrations (1 μg/ 20 μL) were originally used in the sample preparation in the hopes of boosting signal strengths and later the concentrations were decreased in order to find the lowest possible detectability. However, hydroxyl radical production from DHB is higher at the lower concentrations of cholesterol, due to an improved absorbance when the matrix density is at a maximum [57]. Organic matrices were tested at

various concentrations. CHCA exhibited inconvenient results, therefore it was excluded from further tests. Figure 3.1 shows mass spectra of CHCA matrix with 1 mg/mL cholesterol, signal at 369.3 is insignificant.

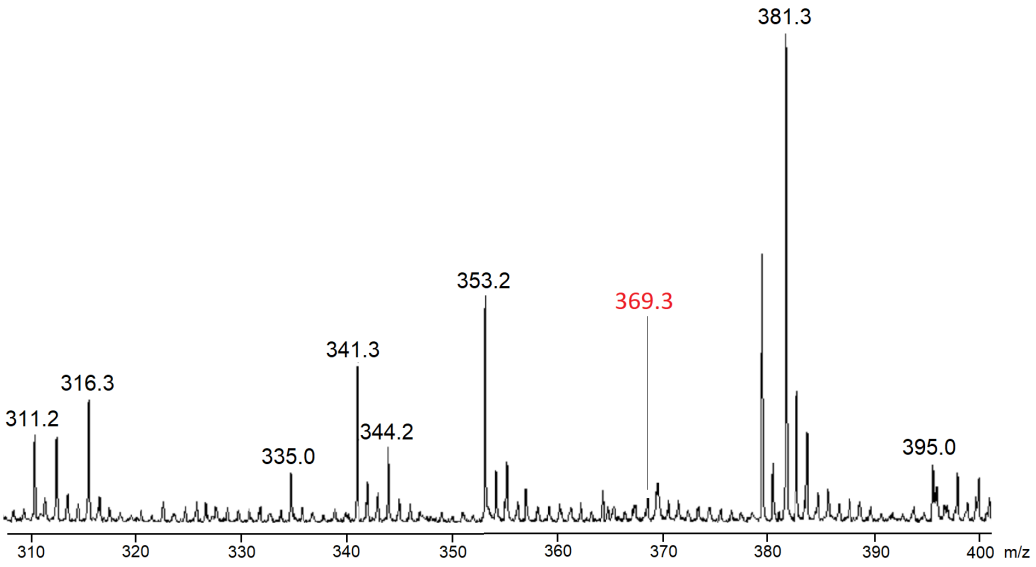

Figure 3.1: Positive ion MALDI TOF mass spectrum of 1 mg/mL cholesterol acquired with CHCA matrix. In red m/z 369.3 for cholesterol peak.

Figure 3.2 represent mass spectra of organic matrices sDHB and DHB (b) and cholesterol acquired with sDHB (c) and DHB (d). The peak at m/z 401 in the MALDI mass spectra represents a solution-based oxidation product of acetonitrile as suggests study conducted by McAvey et al., ACN has been used as a solvent for cholesterol solution. Other signals represent radical cations of oxydated products [57]. Table 3.1 describes signals identified in matrices and signals arising from cholesterol. All samples were applied on MALDI plate in two approaches, first in pre-mix and second in layers, as described in Materials and Methods section. Layer approach showed higher values of S/N of the signal at m/z 369.3 arising from cholesterol. However, this approach is not appropriate due to inhomogeneous co-crystallization of matrix and analyte.

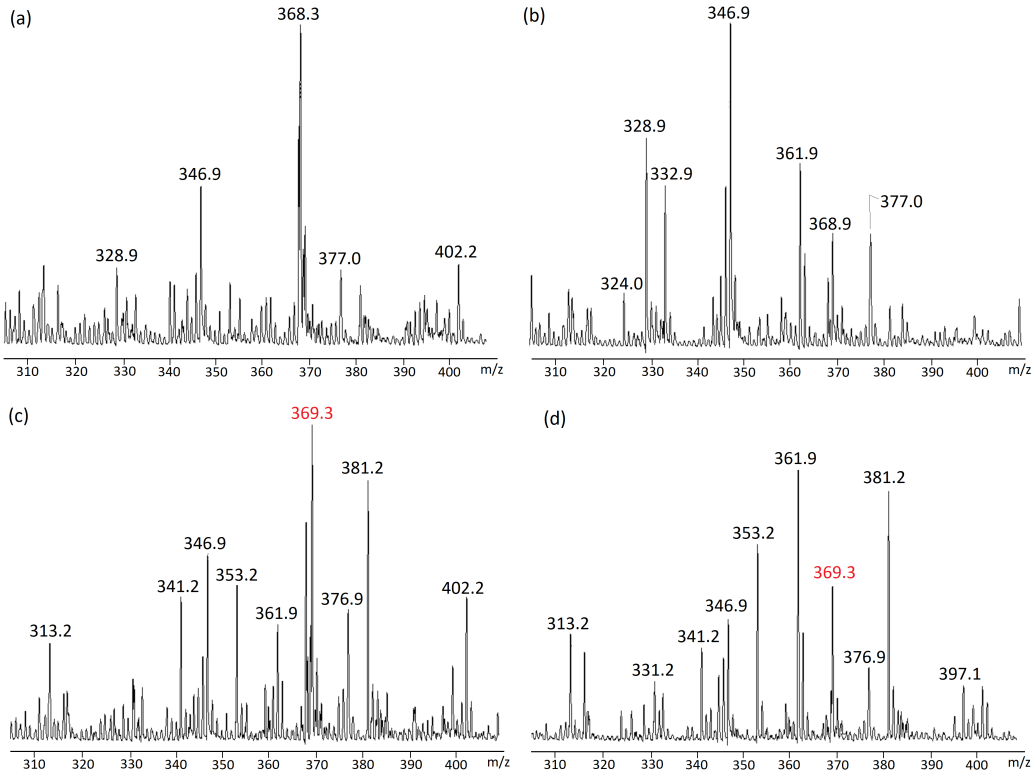

Figure 3.2: Positive ion MALDI TOF mass spectra of organic matrices (a) sDHB and (b) DHB and spectra of cholesterol acquired with matrices (c) sDHB and (d) DHB. The concentration of cholesterol was 15 ng/mL, and the concentrations of organic matrices were 5 mg/mL. All samples were applied in the pre-mix conditions (1:1 volume ratios) and the spectra were acquired with the reflector detector by averaging 2000 individual laser shots at 200 Hz laser frequency. Signals arising from matrices and cholesterol are indicated by m/z ratio.

3.3 Approaches to Overcome Suppression of Signals in Presence of Inorganic Salts

Dozens of nanomaterials have been utilized in nanomaterial-assisted LDI. Considering the inherent advantages, as are unique structure, good performance in optical properties and large surface area, carbon-based nanomaterials have been considered as a good option matrix for laser desorption/ionization to analysis of small molecules. In this work CDs were tested as matrices for the analysis of small molecules as are cholesterol and corti-

costerone. CDs were chosen for their notable characteristics as low toxicity, high stability, easy preparation, low-cost, good biocompatibility, isotropic shapes, chemical inertness, strong absorption coefficient in ultraviolet light (220–350 nm) range what is very important for MALDI TOF MS application, ultra-small size (2–4 nm) which can mitigate the coverage and make the analytes easier to be desorbed. In addition, the abundant carboxylic group on their surface which provides CDs excellent water-solubility and electrical conductivity. In study of Chen [46], CDs showed the highest sensitivity compared with other reported carbon material matrices and they exhibit high salt-tolerance, which is very important in analysis of blood, where is present high amount of salts [46]. To test the efficiency of nanomaterials as assisted matrix for MALDI TOF MS analysis, CDs, N-CDs and GR were examined. Signals identified in positive ion MALDI TOF mass spectra of organic matrices DHB, sDHB, CDs, N-CDs and cholesterol are given in table 3.1.

DHB	**sDHB**	**CDs**	**N-CDs**	**CHOL**
301.0	301.0	331.2	307.1	369.3
304.2	304.2	365.0	353.2	381.2
313.2	316.2		365.0	397.2
316.2	328.9			401.2
326.3	330.9			437.0
328.9	341.2			
332.9	345.9			
341.2	346.9			
344.8	353.2			
345.9	359.9			
346.9	360.9			
353.1	367.9			
361.8	375.0			
368.3	409.9			
500.8	411.9			
	422.0			
	500.9			

Table 3.1: Detected signals in positive ion MALDI TOF mass spectra of organic matrices DHB, sDHB, CDs, N-CDs and cholesterol.

The spectra of cholesterol acquired with CDs, CDs + sDHB, CDs + DHB are presented in Figure 3.3. The DHB matrix with CDs does not show good performance at cholesterol analysis and its spectra exhibits many background signals. At all tested concentrations, sDHB yields higher S/N for the signal

at m/z 369.3 than does DHB. This signal corresponds to the ion generated by the loss of H_2O followed by protonation. Spectra acquired only with CDs without organic matrix exhibits lower number of background signals at m/z range 300 - 400.

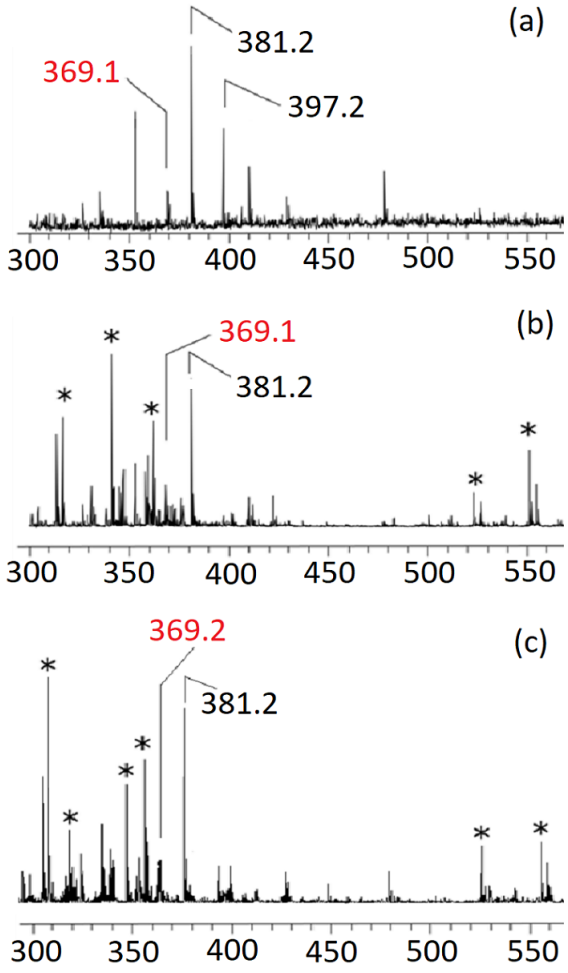

Figure 3.3: Positive ion MALDI TOF mass spectra of cholesterol acquired with (a) CDs, (b) sDHB+CDs and (c) DHB+CDs. [Cholesterol] = 0.095 μM (a, c) and 0.049 μM (b). The signals arising from organic matrices used are indicated by an asterisk, while signals arising from cholesterol and CDs are indicated by their position, i.e. m/z ratio. In red is given m/z for cholesterol peak.

Figure 3.4 shows mass spectra of cholesterol at concentration 0.185 μM acquired with (a) N-CDs, (b) DHB+N-CDs and (c) sDHB+N-CDs. The

number of signals arising from the matrices (indicated by an asterisk in the MS) is lower when N-CDs are used alone as the substrate for MALDI-TOF MS compared to the spectra acquired with organic matrices/nanomaterials binary system. Under all conditions, the signal arising from cholesterol is clearly detectable, although with different intensity. The highest intensity for signal at m/z 369.3 can be observed when N-CDs was used with DHB matrix, however the combination of N-CDs and sDHB show similar pattern.

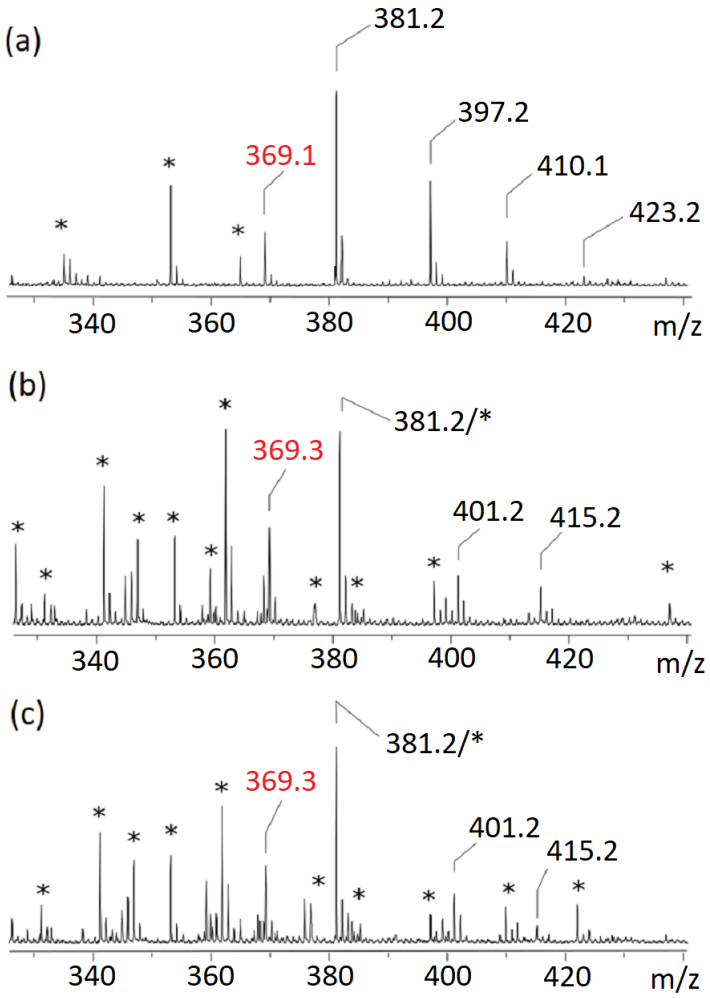

Figure 3.4: Positive ion MALDI TOF mass spectra of cholesterol (0.185 μM) acquired with (a) N-CDs, (b) DHB+N-CDs and (c) sDHB+N-CDs. Matrices were used at concentration of 5 mg/dm^3 and N-CDs 0.5 mg/dm^3. The signals arising from organic matrices are indicated by an asterisk, while signals arising from N-CDs and cholesterol are indicated by m/z ratio.

The spectra of cholesterol obtained with both CDs and N-CDs show mostly background signals, with the S/N ratio > 10, which is around eight times lower than the highest obtained values (in terms of S/N ratio) in the spectra. This suggests that CDs and N-CDs alone are not convenient matrices for the MALDI MS detection of cholesterol, at least in tested concentration range. Contrariwise, after sDHB was used, either alone, or complemented with CDs, the cholesterol signals increased with the concentration (see Figure 3.6).

As can be seen in Figure 3.5, the highest efficiency in detection of cholesterol shows combination of organic matrix sDHB and graphene for concentration of cholesterol 75 ng/mL. As the concentration of cholesterol was decreased, the detection was not possible. Therefore graphene is not ideal assisted matrix for detection of low concentrations presented in sample. However, combination of sDHB and CDs shows good detectability in both concentrations. Zero standard deviation in case of sDHB/CDs also indicates good reproducibility of the method.

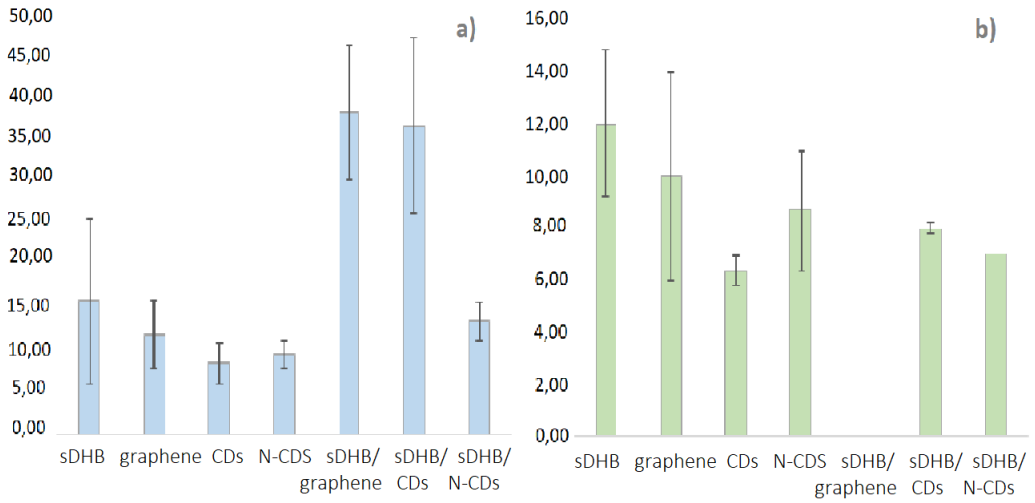

Figure 3.5: Signal-to-noise ratio of the signal at m/z 369.3 arising from cholesterol, acquired with various nanomaterials and the relative standard deviations. Concentration of nanomaterials was 0.3 mg/mL, whereas the concentration of CHO was (a) 75 ng/mL and (b) 3.75 ng/mL.

The best analytical performance with the highest signal-to-noise ratio (S/N) show use of sDHB matrix in combination with 0.3 mg of CDs compared to N-CDs as shows Figure 3.6. N-CDs has mildly increased the number of signals detectable in the mass region of interest.

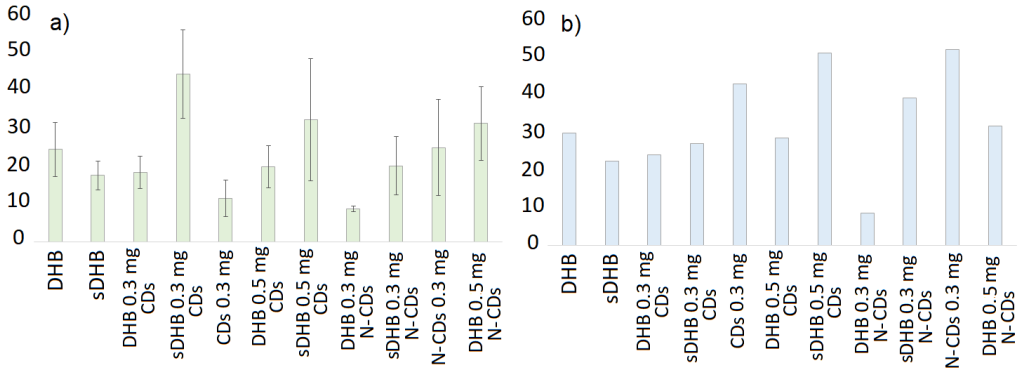

Figure 3.6: S/N of the signal at m/z 369.3 arising from cholesterol, acquired under various conditions (a) and the relative standard deviations (b) expressed as % of the mean value of the S/N. Concentration of CDs and N-CDs was either 0.3 mg/mL or 0.5 mg/mL, whereas the concentration of CHO was 75 ng/mL.

Later on CDs and N-CDs together with/ without DHB and sDHB were tested with and without salts presented in cholesterol sample to observe efficiency in analysis of samples where are salts present, which are the most samples of biological origin. The highest tested concentration was 2% in order to check the detectability. The physiologically relevant concentration, 0.9%, and then concentration 0.4%, 0.2% and 0.1% were tested. Detection of required compound, i.e. corticosterone, by MALDI TOF MS could be difficult because the ion signals of analytes are often suppressed by the presence of a high concentration of salt in biological medium [62]. As shows Figure 3.7, presence of CDs in combination with DHB slightly increased detectability of cholesterol in sample with salt presence. Results are shown in Table 3.2 as the mean value ± SD. Also, RSD expressed as the percentage of the mean value is presented, to check the reproducibility of the method. For both organic matrices used, it was found that even the lowest concentration of NaCl suppressed the signal arising from cholesterol. In some cases, RSD is given as 0, which means that the detectability was not good, or the signal was detected in 1 of 4 wells. Cholesterol was not detected in samples with N-CDs as assisted matrix in combination of organic matrix, also combination of CDs and sDHB was not very effective. The highest detectability was found in samples where N-CDs was applied without organic matrix. Besides, RSD is moderately lower when cholesterol spectra are obtained with the assistance of N-CDs and NaCl. Also, convenient results were obtained by using CDs alone, mean 19.8 for 0.1% and 0.4% NaCl, as indicates Table 3.2. The addition of CDs to the organic matrices recovered the detectability of cholesterol

in the presence of salts, while the addition of N-CDs did not show any improvement of detectability, as can be seen from Table 3.2. The suppression of the analyte signals in the spectra acquired with the organic matrices in the presence of NaCl might be caused by a higher number of signals arising from sDHB compared to DHB, which are even more enhanced by the presence of salts. Moreover, there is possibility of the chemical interactions between carboxyl groups of the benzene ring of DHB and sDHB and amines of N-CDs, that might affect the cholesterol detectability at these conditions [65].

[NaCl] %	**Mean ±SD**	**RSD, %**	**Mean ±SD**	**RSD, %**
	DHB		*sDHB*	
0	19.7 ± 4.1	60.5	33.5 ± 10.2	30.50
0.1	5.5 ± 0	/	0 ± 0	/
0.2	8.0 ± 0	/	0 ± 0	/
0.4	0.0 ± 0	/	0 ± 0	/
0.9	8.0 ± 0	/	0 ± 0	/
2.0	0.0 ± 0	/	0 ± 0	/
	N-CDs		*CDs*	
0	15.3 ± 4.2	27.5	16.0 ± 6.4	39.9
0.1	9.0 ± 2.0	22	19.8 ± 5.1	25.90
0.2	15.5 ± 3.4	22	13.0 ± 3.0	22.70
0.4	22.8 ± 5.6	24.4	19.8 ± 9.1	45.9
0.9	23.8 ± 4.6	19.3	17.8 ± 6.7	37.8
2.0	21.5 ± 5.9	27.5	17.5 ± 4.4	24.90
	sDHB + N-CDs		*sDHB+CDs*	
0.1	0 ± 0	/	8 ± 0	/
0.2	0 ± 0	/	7 ± 0	/
0.4	0 ± 0	/	0 ± 0	/
0.9	0 ± 0	/	8.7 ± 0.6	6.70
2.0	0 ± 0	/	16.0 ± 4.10	25.50
	DHB + N-CDs		*DHB+CDs*	
0.1	0 ± 0	/	16.0 ± 4.1	25.1
0.2	0 ± 0	/	8.0 ± 0.0	/
0.4	0 ± 0	/	9.0 ± 3.5	38.50
0.9	0 ± 0	/	11.7 ± 2.5	21.60
2.0	0 ± 0	/	7.7 ± 1.5	19.90

Table 3.2: S/N ratio of the signal arising from cholesterol at m/z 369.3 detected with sDHB, DHB, CDs, N-CDs, or their combination under increasing content of NaCl.

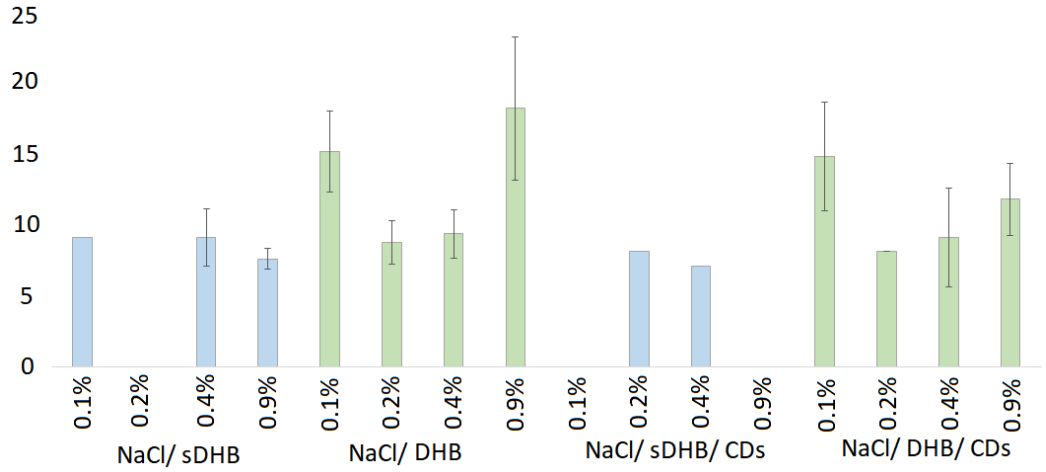

Figure 3.7: Signal-to-noise ratio of the signal at m/z 369.3 arising from cholesterol acquired under various conditions with the relative standard deviations. Cholesterol samples contain NaCl solution in range 0.1 - 0.9%. Concentration of CDs was 0.3 mg/mL, whereas the concentration of cholesterol was 15 ng/ 200 μL.

Figure 3.8 shows mass spectra of cholesterol with addition of NaCl (0.9%) obtained with CDs and N-CDs. In case of CDs use, the peak of cholesterol is distincter than in case of N-CDs, however there is lot of signals from CDs matrix that suppress signals from cholesterol.

COOH and NH_2 groups that can be found on the surface of CDs help to improve the detection of cholesterol by MALDI MS in the presence of inorganic cations. The enhancing effect of CDs is due to a negative Gibbs energy of the complex formation between CDs, DHB, Na^+ and cholesterol [65].

Even though carbon-based nanomaterials demonstrated a high potential for detection of cholesterol in the presence of high salt concentrations, there are still some drawbacks of their applications as substrates for MALDI TOF MS. These drawbacks are associated with their optical properties, electroconductivity and homogeneity of distribution on the sample plate. Some studies suggest the use of coated MALDI plates instead of nanoparticles to achieve better homogeneity of sample/particle distribution, however, these plates are not yet available enough on the market and their purchase price is too high for many institutions, therefore their application was excluded from this work. The method for CS concentration was, thus, developed only with the use of organic matrices.

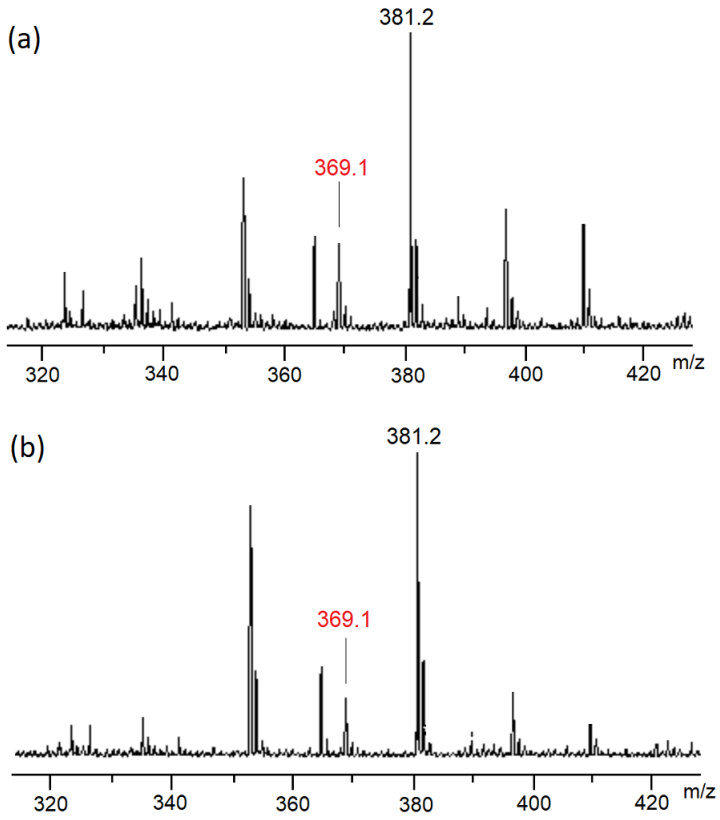

Figure 3.8: Positive ion MALDI TOF mass spectra of cholesterol (15 ng/mL) and NaCl (0.9 %) acquired with (a) CDs and (b) N-CDs. Signals arising from cholesterol are indicated by m/z ratio.

3.4 Detection of Corticosterone by MALDI TOF MS

As the outcome of results obtained in previous chapter, MALDI possess the potential for detection of small molecules. Therefore, in the next part, the stress hormone corticosterone was analysed by MALDI MS. Signals arising from DHB, sDHB, CHCA and corticosterone are shown in Table 3.3. The major ion peak for corticosterone was found to be m/z 347, which corresponds to the proton adduct , i.e. (M+H)+. The positive ion mass spectra of corticosterone in ACN/MetOH acquired with DHB are given in Figure 3.9. Samples were prepared by dried-droplet method. Figure 3.9, spectrum (a), shows corticosterone with labeled internal standard in final concentration of 2.5 mg/mL with DHB matrix, whereas (b) shows spectrum without internal

DHB	sDHB	CHCA	CS
308.2	331.2	317.3	318.5
313.2	332.5	318.2	329.4
315.2	368.6	319.3	330.5
326.5	412.6	326.5	346.2
329.2	422.7	332.5	347.4
331.2	428.7	333.2	374.6
332.5		335.2	
338.5		337.2	
340.5		343.4	
341.5		360.5	
346.1		361.2	
347.2		362.2	
353.5		363.2	
359.5		364.8	
362.2		379.2	
368.6		380.3	
381.5			

Table 3.3: Detected signals in positive ion MALDI TOF mass spectra of organic matrices DHB, sDHB, CHCA and corticosterone.

standard. Both spectra display signals of corticosterone with background noise arising from DHB matrix. Spectra of DHB matrix alone is shown in (c). The highest signal of DHB is at m/z 332, m/z 353, m/z 369 and m/z 381.

Figure 3.10 shows spectra of corticosterone sample with sDHB matrix. Image (a) represents spectra of corticosterone with labeled IS in final concentration of 2.5 mg/mL with sDHB matrix, image (b) displays spectra of 2.5 mg/mL corticosterone with sDHB and at (c) is sDHB matrix alone. Spectrum (b) exhibits higher background noise than spectrum (a). The strongest signals arising from sDHB matrix are at m/z 332, m/z 368 and m/z 402.

The spectra of corticosterone acquired with CHCA is given in Figure 3.11. Corticosterone with labeled internal standard in final concentration of 2.5 mg/mL with CHCA matrix represents image (a), corticosterone with concentration 2.5 mg/mL with CHCA matrix (b) and spectra of CHCA matrix is shown in (c). The main signals arising from CHCA matrix are at m/z 335 and at m/z 379. In case of use CHCA matrix, the signals arising from corticosterone at m/z 347.4 are easily detectable and the background noise is negligible.

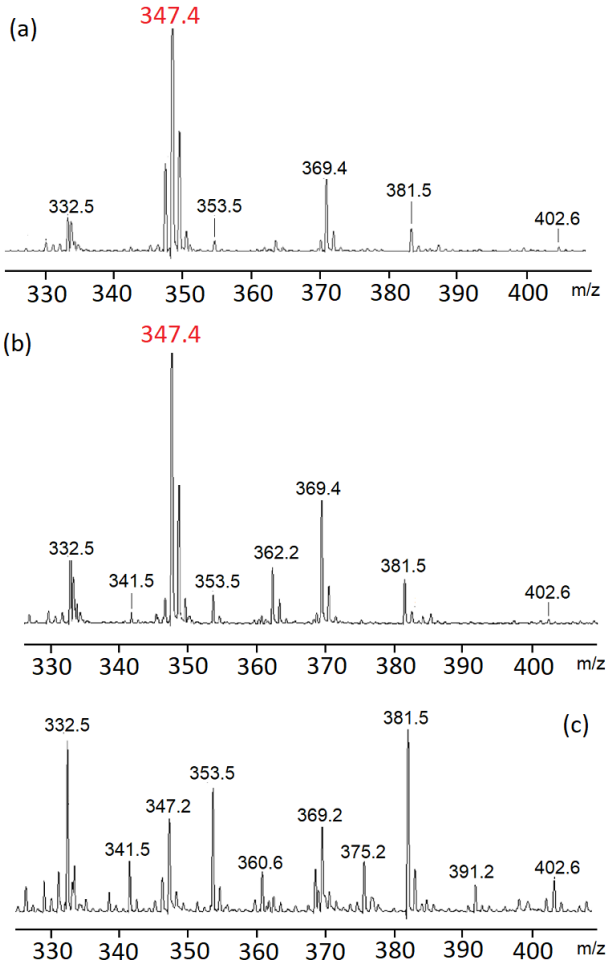

Figure 3.9: Positive ion MALDI TOF mass spectra of (a) CS with labeled IS of final concentration 2.5 mg/mL with DHB matrix, (b) CS with concentration 2.5 mg/mL with DHB matrix, and (c) signal arising from DHB matrix. All samples were applied by dried-droplet method. Signals arising from CS are at m/z 347.4.

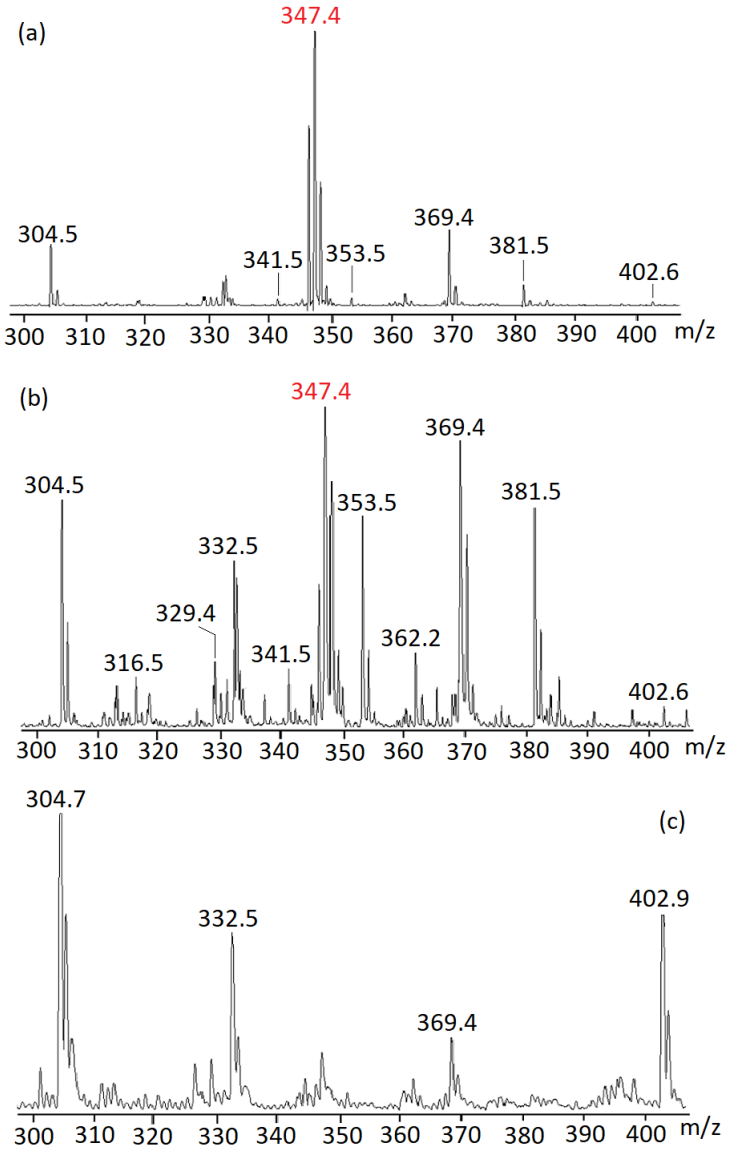

Figure 3.10: Positive ion MALDI TOF mass spectra of (a) corticosterone with labeled internal standard of final concentration 2.5 mg/mL with sDHB matrix, (b) corticosterone with concentration 2.5 mg/mL with sDHB matrix, and (c) signal arising from sDHB matrix. All samples were applied by dried-droplet method. Signals arising from corticosterone are at m/z 347.4.

Other signals arise from oxidation products and extraction buffer ACN/MetOH, these are: at m/z 304, 369, 401, 402, 410. It is not possible to detect signals arising from IS due to proximity of matrix signal at m/z 353 and also suppression of the signal of IS which is at m/z 351.4.

3.5 Testing the Possibility of Corticosterone Quantification

As this is a new approach to analyse corticosterone by MALDI-TOF MS and MALDI is not a routine method used for quantification of small molecules, necessary tests were conducted. As a quantitation approach for reaction profiling using MALDI-MS was used an isotopically labeled internal standard similar to corresponding hormone, in this cause Corticosterone-9,11,12,12-d_4 98 atom % D, 97% (CP) with molecular weight 350.49. This method is convenient for reaction optimization with a single product across the whole plate [47], which is at this case corticosterone. As internal standard, this labeled compound has the same ionization properties (the same number of ions in the spectra as CS), same polarity (miscibility with matrices) and similar mass, which is important for possible quantification of compounds by MALDI TOF MS [77]. The concentration of IS was kept constant, 10 μg/mL, mixed with CS and dissolved with ACN/MetOH solution to final concentration of CS in range from 0.16 to 5 mg/mL. Spectra were acquired with CHCA, DHB and sDHB matrices. The MS signal intensity was compared with samples spiked with IS and without IS. All samples were prepared in quadruplicates and measurements done in three consecutive days in order to obtain day-to-day reproducibility and within-day precision.

The quantification was achieved with the regression equation derived from the calibration curve. Figure 3.12 shows linear curves of corticosterone samples in range from 0.16 - 5 mg/mL with different matrices and measurements of each day. The detector response is given in S/N ratio. The linearity equations are presented in the figures. The linearity differs from day to day within one matrix measurements. The most variable results are observed for sDHB matrix. It should be mentioned that not all signals were detected under all acquisition conditions and at all tested concentrations.

Figure 3.13 presents linearity curves of CS spiked with IS, concentration range from 0.16 - 5 mg/mL. The linearity was demonstrated similarly for all matrices and measurements. The most apparent differences are between day 1, $R^2 = 0.9854$, slope = 2.9132, intercept = -0.5546, and day 2, $R^2 = 0.9949$, slope = 1.9827, intercept = 0.2495 for CHCA matrix.

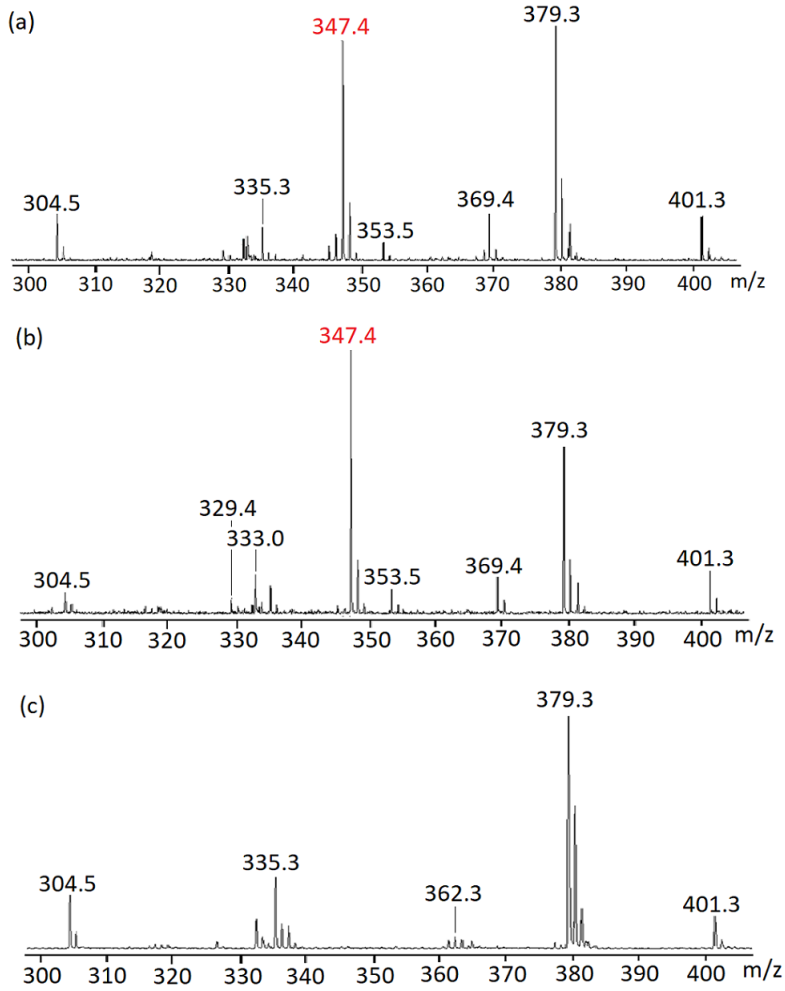

Figure 3.11: Positive ion MALDI TOF mass spectra of (a) corticosterone with labeled internal standard of final concentration 2.5 mg/mL with CHCA matrix, (b) corticosterone with concentration 2.5 mg/mL with CHCA matrix, and (c) signal arising from CHCA matrix. All samples were applied by dried-droplet method. Signals arising from corticosterone are at m/z 347.4.

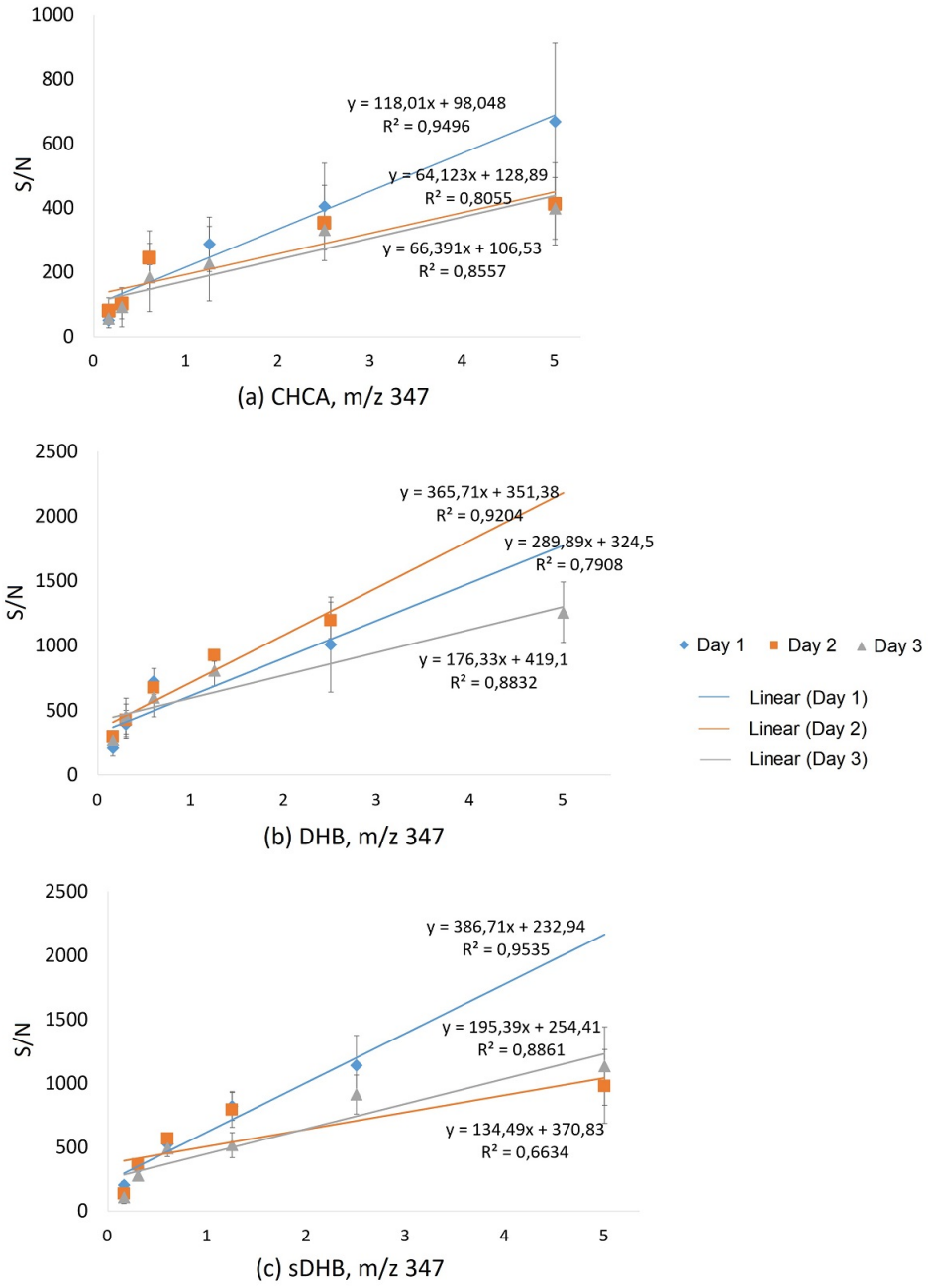

Figure 3.12: Detectability and comparison of linearity of corticosterone detection with different matrices, (a) CHCA, (b) DHB and (c) sDHB, calculated based on the mean S/N ratio of CS signal at 347.4 for each set of measurements with standard deviations. Concentrations of CS are from 0.16 - 5 mg/mL. Linearity equations are indicated in the graph.

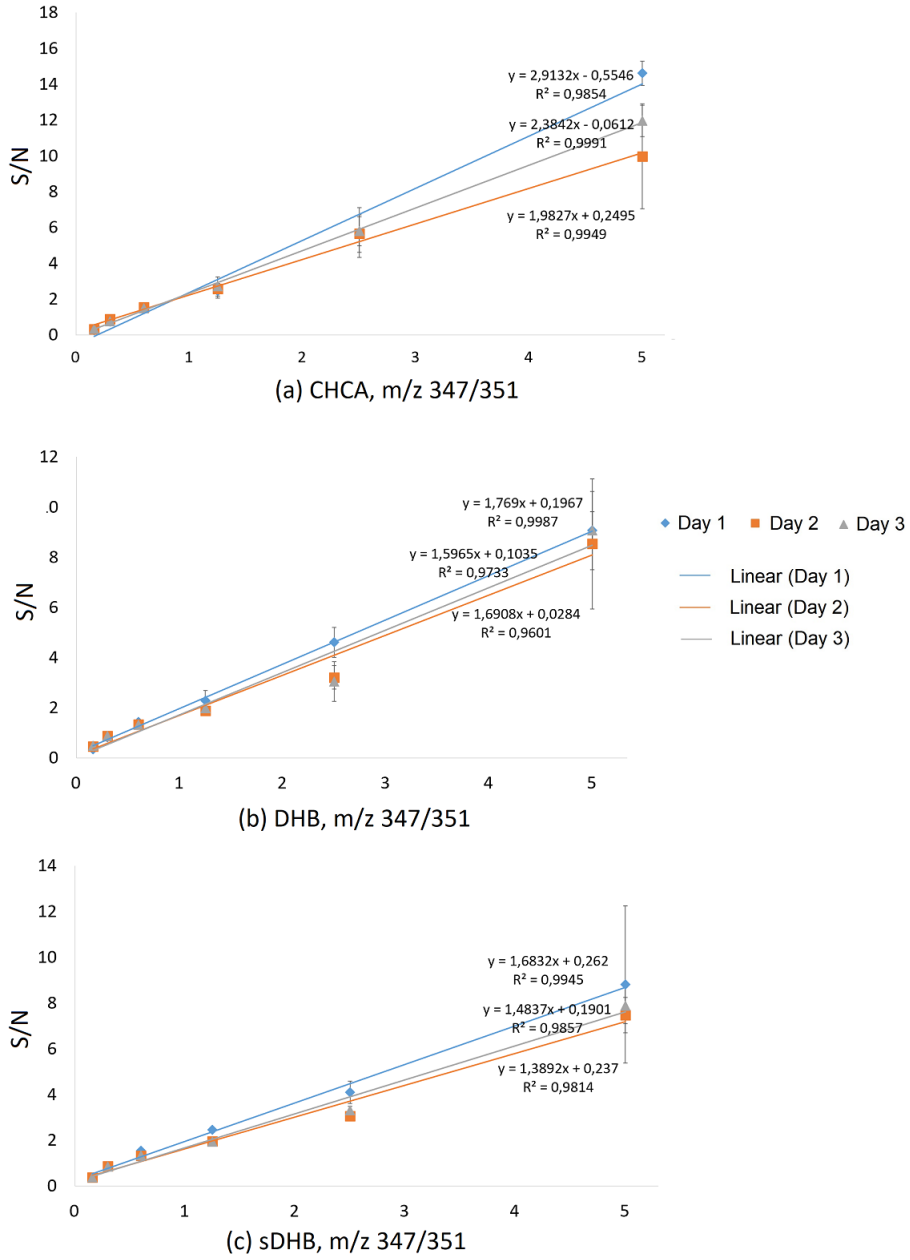

Figure 3.13: Detectability and comparison of linearity of corticosterone detection spiked with isotopically labeled IS, with different matrices, (a) CHCA, (b) DHB and (c) sDHB, calculated based on the mean S/N ratio of CS signal at 347.4/351.4 for each set of measurements with standard deviations. Concentrations of CS are from 0.16 - 5 mg/mL. Linearity equations are indicated in the graph.

Figure 3.14 presents the response of the detector for the signal at m/z 347.4 and at 347.4/351 in case of samples spiked with IS, graphs show linearity and the mean values of three day measurements with standard deviations. The sensitivity of detection is higher with correction factor, i.e. in the case when corticosterone is spiked with IS, and standard deviations are smaller. Addition of internal standard is effective in improvement of reproducibility of the spectra and for the measurements of quantification. In case when a correction factor is used, all three used matrices show similar pattern and linearity is achieved. Standard deviations are smaller for lower concentrations which can be also caused by lower S/N ratio. The most linear pattern was found for CHCA matrix spiked with IS, $R^2 = 0.998$, slope = 2.4266, intercept = -0.121. For DHB with IS, $R^2 = 0.985$, slope = 1.6853, intercept = 0.1107, and sDHB matrix with IS has $R^2 = 0.989$, slope = 1.5201 and intercept = 0.2201.

Table 3.4 shows the values for the limit of detection (LOD), the limit of quantification (LOQ), coefficient of determination (R^2). The values represent statistically processed S/N values detected in the corticosterone spectra with range of concentrations from 0.16 to 5 mg/mL acquired both with and without IS, and with three different matrices CHCA, DHB and sDHB. The measurements were performed for three consecutive days. In all analyzed samples the values of concentration for LOD and LOQ are lower when IS was used. For example, the values in case of use of sDHB matrix in day 1 are very distinct, LOD for sample with IS is 10.05 and without IS only 0.46. The same pattern follows all other measurements. The lowest value of LOD, 0.19, was found in sample with IS, day 3, and CHCA matrix. When mean values of concentrations for three days of measurement were analyzed, it can be seen that values were similar for all applied matrices. The lowest concentration for the S/N at m/z 347.4 and for the S/N ratios at m/z 347.4 and at m/z 351.4 were detected with CHCA as matrix (2.90 mg/mL and 0.33 mg/mL, respectively), so internal standard increase sensitivity almost ten times. The values for coefficient of determination are higher when IS was used, and linearity was demonstrated, R^2=0.998 for CHCA, R^2=0.985 for DHB and R^2=0.989 for sDHB, all samples with IS, summary of all three days measurements (D1-D3). Values of coefficient of determination for samples without IS are slightly lower, R^2=0.822 for CHCA, R^2=0.769 for DHB and R^2=0.951 for sDHB. Table **??** shows the linear equation with determined values for slope and intercept for the S/N values (signals at 347.4 and ratio be-tween signals at 347.4 and at 351.4) detected in the corticosterone spectra acquired both without and with IS with different concentrations, and with three different matrices CHCA, DHB and sDHB, for three consecutive days of measurements.

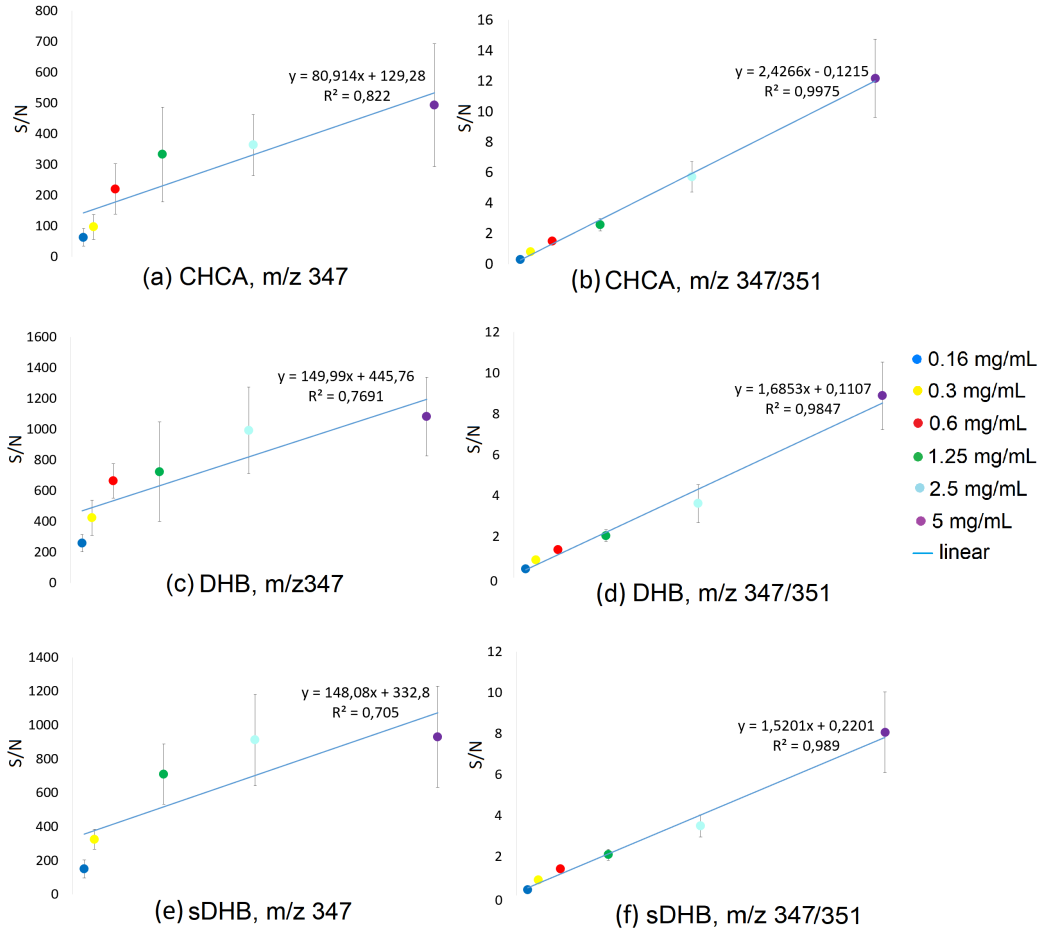

Figure 3.14: Comparison of linearity of corticosterone and corticosterone spiked with IS, with different matrices, (a, b) CHCA, (c, d) DHB and (e, f) sDHB, calculated based on the mean S/N ratio of CS signal at 347.4 and at 347.4/351.4 in case of IS, the mean values of 3 days measurements with standard deviations. Concentrations of CS are from 0.16 - 5 mg/mL. Linearity equations are indicated in the graph.

N_o Day	S/N	parameters	CHCA	DHB	sDHB
D1	347	LOD	1.44	4.55	10.05
		LOQ	4.78	15.17	33.51
		R^2	0.946	0.791	0.954
	347/351	LOD	0.78	0.23	0.46
		LOQ	2.53	0.76	1.54
		R^2	0.985	0.999	0.994
D2	347	LOD	8.53	6.22	4.61
		LOQ	28.44	20.77	15.36
		R^2	0.805	0.920	0.66
	347/351	LOD	0.45	1.03	0.86
		LOQ	1.49	3.44	2.86
		R^2	0.999	0.960	0.981
D3	347	LOD	2.56	2.35	2.23
		LOQ	8.53	7.84	7.44
		R^2	0.856	0.883	0.886
	347/351	LOD	0.19	1.27	0.75
		LOQ	0.64	4.23	2.50
		R^2	0.995	0.973	0.987
D1-D3	347	LOD	2.90	3.41	4.15
		LOQ	9.66	11.38	13.85
		R^2	0.822	0.769	0.951
	347/351	LOD	0.33	0.78	0.66
		LOQ	1.11	2.59	2.19
		R^2	0.998	0.985	0.989

Table 3.4: The calculated values (ANOVA analysis, regression) for the limit of detection (LOD), the limit of quantification (LOQ), coefficient of determination (R squared, R^2), for the S/N values (signals at 347.4 and ratio between signals at 347.4 and at 351.4) detected in the corticosterone spectra acquired both without and with IS with different concentrations, and with three different matrices CHCA, DHB and sDHB, for three consecutive days of measurements.

N_o Day	S/N	CHCA	DHB	sDHB
D1	347	y=118.01x+98.048	y=289.89x+324.5	y=386.71x+232.94
	347/351	y=2.9132x-0.5546	y=1.769x+0.1967	y=1.6832x+0.262
D2	347	y=64.123x+128.89	y=365.71x+351.38	y=134.49x+370.83
	347/351	y=2.3842x-0.0612	y=1.6908x+0.0284	y=1.3892x+0.237
D3	347	y=66.391x+106.53	y=176.33x+419.1	y=195.39x+254.41
	347/351	y=1.9827x+0.2495	y=1.5965x+0.1035	y=1.4837x+0.1901
D1-D3	347	y=80.914x+129.28	y=149.99x+445.76	y=0.3168x-20.419
	347/351	y=2.4266x-0.1215	y=1.6853x+0.1107	y=1.5201x+0.2201

Table 3.5: The linear equations with determined values for slope and intercept, for the S/N values (signals at 347.4 and ratio between signals at 347.4 and at 351.4) detected in the corticosterone spectra acquired both without and with IS with different concentrations, and with three different matrices CHCA, DHB and sDHB, for three consecutive days of measurements.

To investigate and evaluate the relative quantification capacity and accuracy of the designed method for routine laboratory application, one way analysis of variance (ANOVA) was used, and the F parameters (both determined F and Fcrit) were obtained. The differences between three days of measurements for the sample of corticosterone without and with internal standards with five different concentrations were evaluated with ANOVA. With this method the null hypothesis is tested, if the mean values of three days are equal, or at least not significantly different. Before this test, the Grubbs test for outliers was performed for all the results for each day, and then mean values which are acceptable were used for further calculations.

The precision of the method was determined by comparison of the within-day precision and day-to-day reproducibility within three days of the spectra acquisition. Table 3.6 represent values of day-to-day repeatability and within day precision processed by ANOVA test. The results indicate that the most of coefficient of variations have the values lower than 20% in case when internal standard was used. These values are acceptable as the lowest level of quantification should not exceed 20%. The values of variation without internal standards are slightly higher, and most of them exceed 20%. The best results were found in case of use of DHB and sDHB with IS, when the values are in most cases lower than 10%, it indicates that the reproducibility of the method is very high and also potential for the quantitative analysis is promising. The lowest value, 2.2%, was achieved for 0.3 mg/mL of corticosterone with DHB matrix spiked with IS when within-day precision was calculated. Similar results (2.7%) are given for sDHB matrix. Also concen-

mg		**ANOVA Day to day, %** *CHCA*	*DHB*	*sDHB*	**ANOVA Within day, %** *CHCA*	*DHB*	*sDHB*
0.16	347	12.3	18.8	35.0	44.7	16.7	24.2
	347/351	13.4	18.1	*5.5*	*8.5*	*9.5*	10.4
0.3	347	25.9	14.5	12.5	46.1	29.2	15.6
	347/351	8.0	*4.0*	*3.0*	11.0	*2.2*	*2.7*
0.6	347	14.6	*5.1*	*4.1*	38.5	16.4	11.6
	347/351	*3.0*	*4.8*	*8.6*	*3.0*	*3.4*	*2.6*
1.25	347	46.7	33.8	25.6	25.2	37.1	16.4
	347/351	*7.6*	*9.1*	14.3	16.2	12.1	*6.2*
2.5	347	11.5	20.0	30.2	28.5	24.2	19.4
	347/351	11.1	25.4	17.1	19.4	17.5	*9.2*
5.0	347	29.4	*9.7*	24.4	34.3	22.6	26.5
	347/351	20.4	11.0	11.3	14.8	20.2	25.9

Table 3.6: The values of day to day repeatability and within day precision, calculated with ANOVA tools, for the S/N values (signals at 347.4 and ratio between signals at 347.4 and at 351.4) detected in the corticosterone spectra acquired without and with IS with concentrations from 5 - 0.16 mg/mL, and with matrices CHCA, DHB and sDHB. Red numbers show results with values below 5%.

tration 0.6 mg/mL of corticosterone with all three matrix spiked with IS when within-day precision was calculated, exhibits good results, 3.0% for CHCA, 3.4% for DHB and 2.6% for sDHB. CS concentration of 0.6 mg/mL spiked with IS when day-to-day repeatability was calculated achieved 3.0%. For the lowest concentration of CS (0.16 mg/mL) the best within day repeatability was obtained with DHB matrix (16.7%), similar results was obtained for the day-to-day repeatability with DHB matrix (18.8%). Samples of the lowest concentrations of CS spiked with IS exhibits lower values of variations.

F values were obtained by ANOVA test processed in Excel program. F critical values (Fcrit) are determined from the statistical tables, which represent the upper critical values of the F distribution with the precision degree 95% and the factor α=0.05 for certain number of measurements. Table 3.7 shows the F and Fcrit values for signals at 347.4 and at 347.4/351.4 detected in corticosterone mass spectra acquired with and without IS and with different matrices. In cases where number is indicated by red color, the variations in groups have significant differences, and they are higher than variations between groups, as well as null hypothesis is rejected and the mean values

mg		**F** *CHCA*	*DHB*	*sDHB*	**Fcrit** *CHCA*	*DHB*	*sDHB*
0.16	347	1.22	4.78	7.23	4.26	4.26	4.26
	347/351	8.43	11.95	0.18	4.46	4.26	4.26
0.3	347	0.05	0.26	2.93	4.26	4.26	4.26
	347/351	2.56	11.33	4.73	4.46	4.26	4.26
0.6	347	0.57	1.29	1.37	4.46	4.26	4.46
	347/351	4.05	6.91	33.60	4.26	4.26	4.46
1.25	347	11.29	3.49	8.34	4.46	4.26	4.26
	347/351	0.35	2.70	17.07	4.46	4.46	4.46
2.5	347	0.51	3.06	8.25	4.26	4.26	4.46
	347/351	0.01	7.36	11.32	4.26	4.26	4.26
5.0	347	3.20	1.55	3.53	4.26	4.26	4.26
	347/351	6.64	0.12	0.43	4.26	4.26	4.26

Table 3.7: The F and Fcrit values, determined by an ANOVA test, for signals at 347.4 and ration between signals at 347.4 and at 351.4 detected in the corticosterone spectra acquired without and with internal standard with different concentrations and different matrices. When the value of F is higher than value of Fcrit, the number is written in red.

are not equal. In case of sDHB matrix, the null hypothesis is rejected for most of tested concentrations for both without IS and with IS measurements. On the contrary, CHCA matrix exhibits promising results when in most of concentrations the values fail to reject null hypothesis.

In order to obtain the overview of statistical calculations and the main details of descriptive statistics the box-and-whisker plots were created. Figure 3.15 shows box-and-whisker plot (a) for the S/N values at m/z 347.4 and (b) for the ratio of signals at m/z 347.4 and m/z 351.4 at the concentration of corticosterone 0.6 mg/mL with matrices CHCA, DHB and sDHB. On the diagram up and bottom of box are defined with first quartile (Q1) and third quartile (Q3). The first quartile is the middle value between the smallest number (minimum) and the median of the data set. The third quartile is defined as the middle number between the median and the highest value (maximum) of the data set. The median S/N values for the signal at m/z 347.4 are 220 for CHCA, 671 for DHB and 540 for sDHB matrix. In case of CHCA matrix the upper extreme is 386 and the lower extreme is 90, for DHB the upper value is 987 and the lower is 377, for sDHB the upper extreme is 711 and the lower extreme is 319. The median S/N values for the signal at m/z 347.4/351.4 are 1.5 for CHCA, 1.3 for DHB and 1.3 for sDHB.

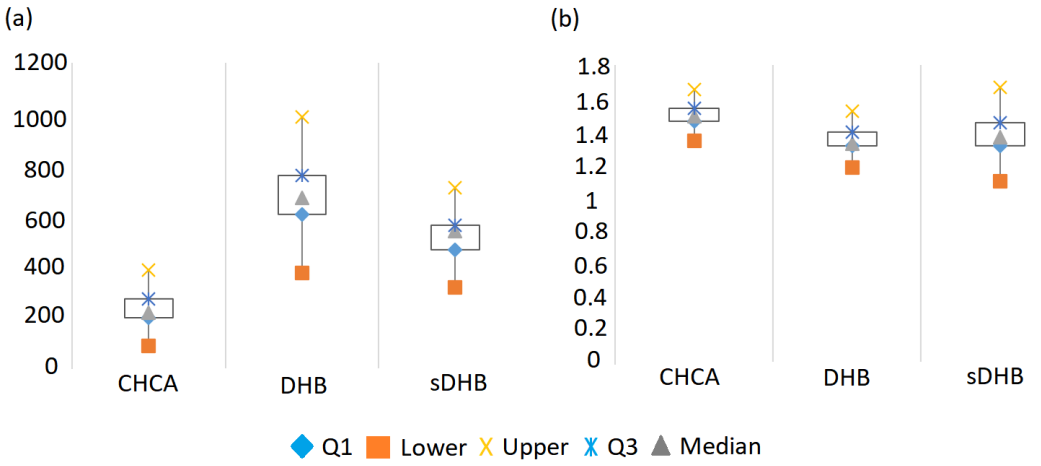

Figure 3.15: Box and whiskers plot of the data obtained from the S/N values for the signal (a) at m/z 347.4 and (b) for the ratio of signals at m/z 347.4 and m/z 351.4 for the concentration 0.6 mg/mL of the corticosterone with matrices CHCA, DHB and sDHB.

The upper/lower extreme is 1.7/1.3 for CHCA, 1.5/1.2 for DHB and 1.7/1.1 for sDHB. The lower and upper values are deviations within measurements (external values).

These results confirm above mentioned calculations, correction with internal standard gives more homogenous results, with less width spread results with smaller values of deviations. The use of an internal standard also shows smaller variations between the use of different matrices. It is shown that MALDI has the potential for detection and pontificating of CS as the stress indicator in turtles.

3.6 Detection and Quantification of CS in Turtle's Plasma

Last part of this work was to investigate the sensitivity and accuracy of the detection of corticosterone in turtle's plasma. Corticosterone was extracted from plasma, mixed with matrices and analysed by MALDI-TOF MS. Corticosterone was not detected in plasma, it might be due to various reasons, as are: the corticosterone level in plasma sample might be too low to be detected, CS recovery rate is too low, or this method is not sensitive enough to detect lower values of corticosterone, as the values of CS in turtle's plasma range between 0.05 to 25.15 ng/mL [38]. Figure 3.16 shows spectra of plasma

sample after extraction procedure acquired with DHB matrix. At m/z 347.4 was not detected any signal, the same measurements were conducted with sDHB and CHCA matrices with the same results.

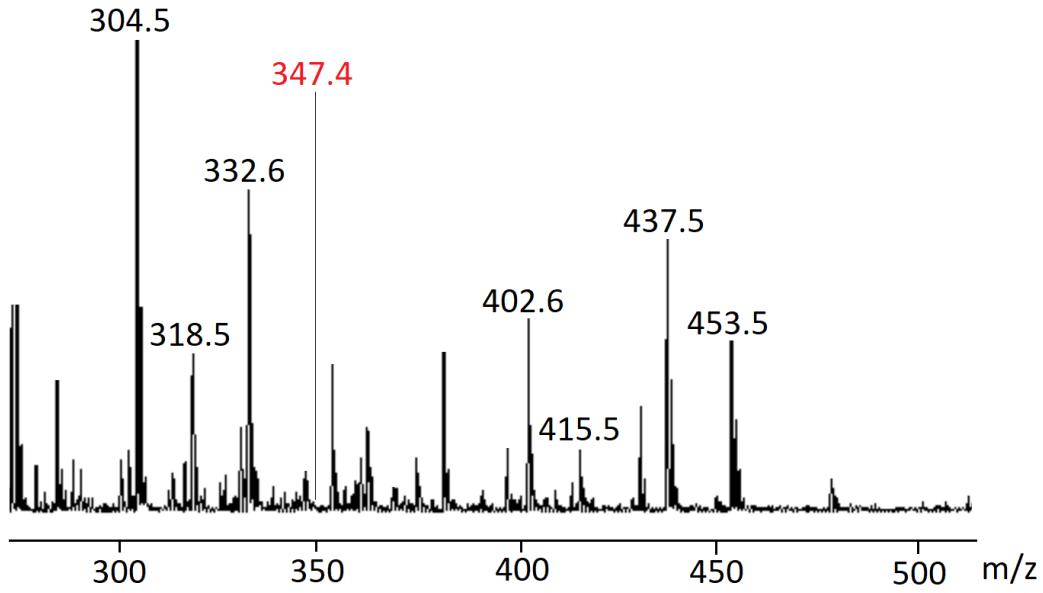

Figure 3.16: Positive ion MALDI TOF mass spectra of plasma sample after extraction of corticosterone with DHB matrix. There are no signals arising from corticosterone at m/z 347.4, expected signal is indicated by m/z ratio.

In order to test the ability to detect CS in plasma and assure there was no error during extraction procedure, the CS in range 39 μg/mL to 5 mg/mL was added to plasma sample before extraction. Samples were extracted following precisely the extraction procedure. Another set of samples were spiked with IS, which have been used as as a correction factor and, to check the recovery of CS from the blood and for potential quantification. The measurements were performed for three consecutive day to observe day to day reproducibility, within day precision and obtain statistical significance, in analogous manner as described in the previous chapter.

Figure 3.17 represents mass spectra of extracted plasma sample with added 2.5 mg/mL CS and another spectra spiked with IS with final concentration of CS 2.5 mg/mL acquired with CHCA matrix. Signal at m/z 347.4 is easy detectable, when sample is spiked with IS, signal is stronger, however surrounding signals are stronger as well. Strong signal is arising at m/z 353.5. Also, there is strong background noise, which arises most likely from the variety of co-extracted components from the blood.

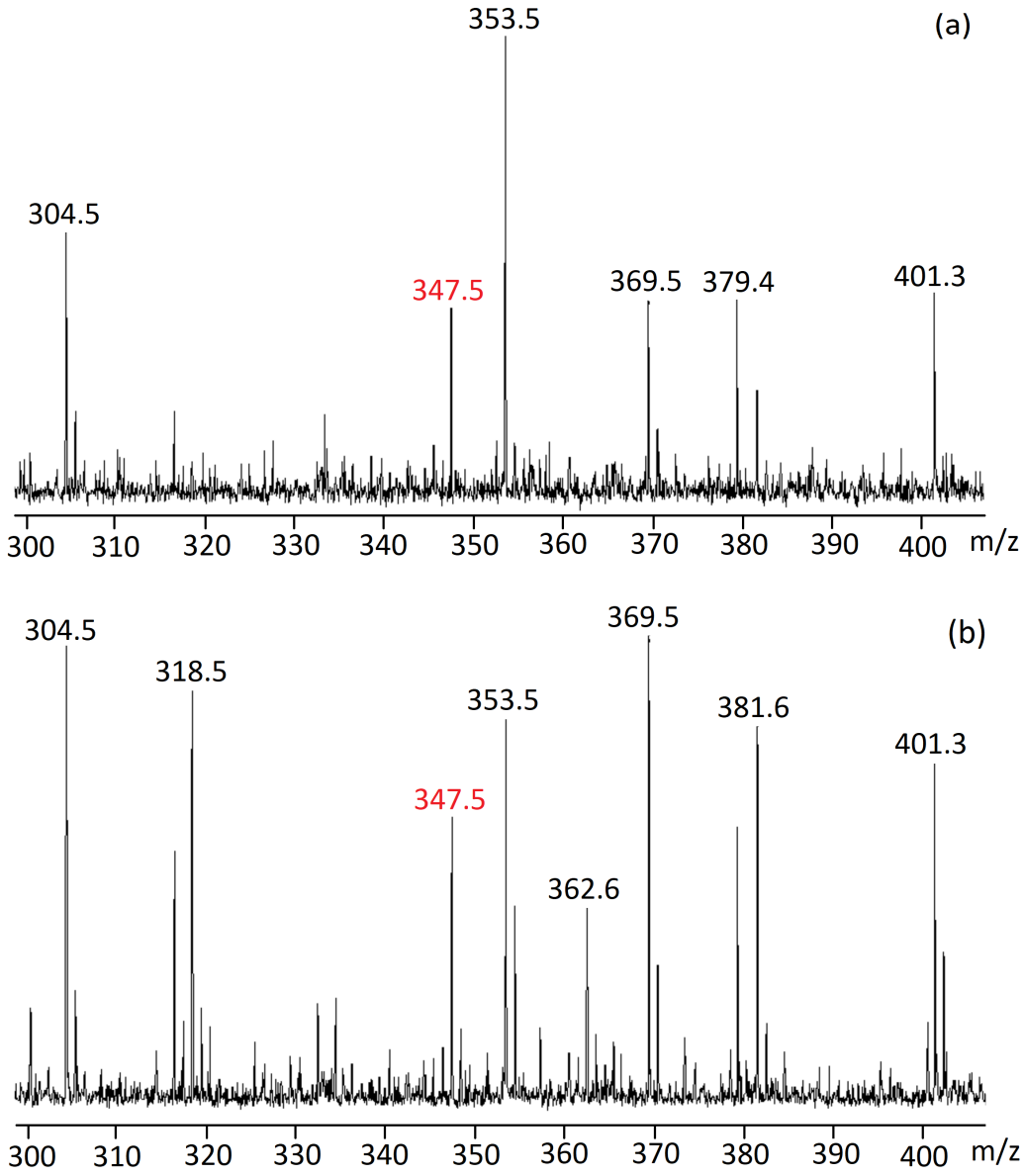

Figure 3.17: Positive ion MALDI TOF mass spectra of extracted turtle's plasma with added (a) corticosterone 2.5 mg/mL with CHCA matrix and (b) corticosterone with labeled internal standard of final concentration 2.5 mg/mL with CHCA matrix.

The same measurements were done with DHB matrix, the results are same as in case of CHCA (spectra are displayed in Figure 3.18). Signal at m/z 347.4 was detected in both spectra, but in the spectra with IS (b) there

is additional low intensity signal at m/z 351.5, that arises from the proton adduct of IS. At spectra spiked with IS is the signal at m/z 347.4 stronger, in both cases is surpassed by signal at m/z 353.5, which arises from matrix. Compared with CHCA matrix, DHB matrix has smaller background noise.

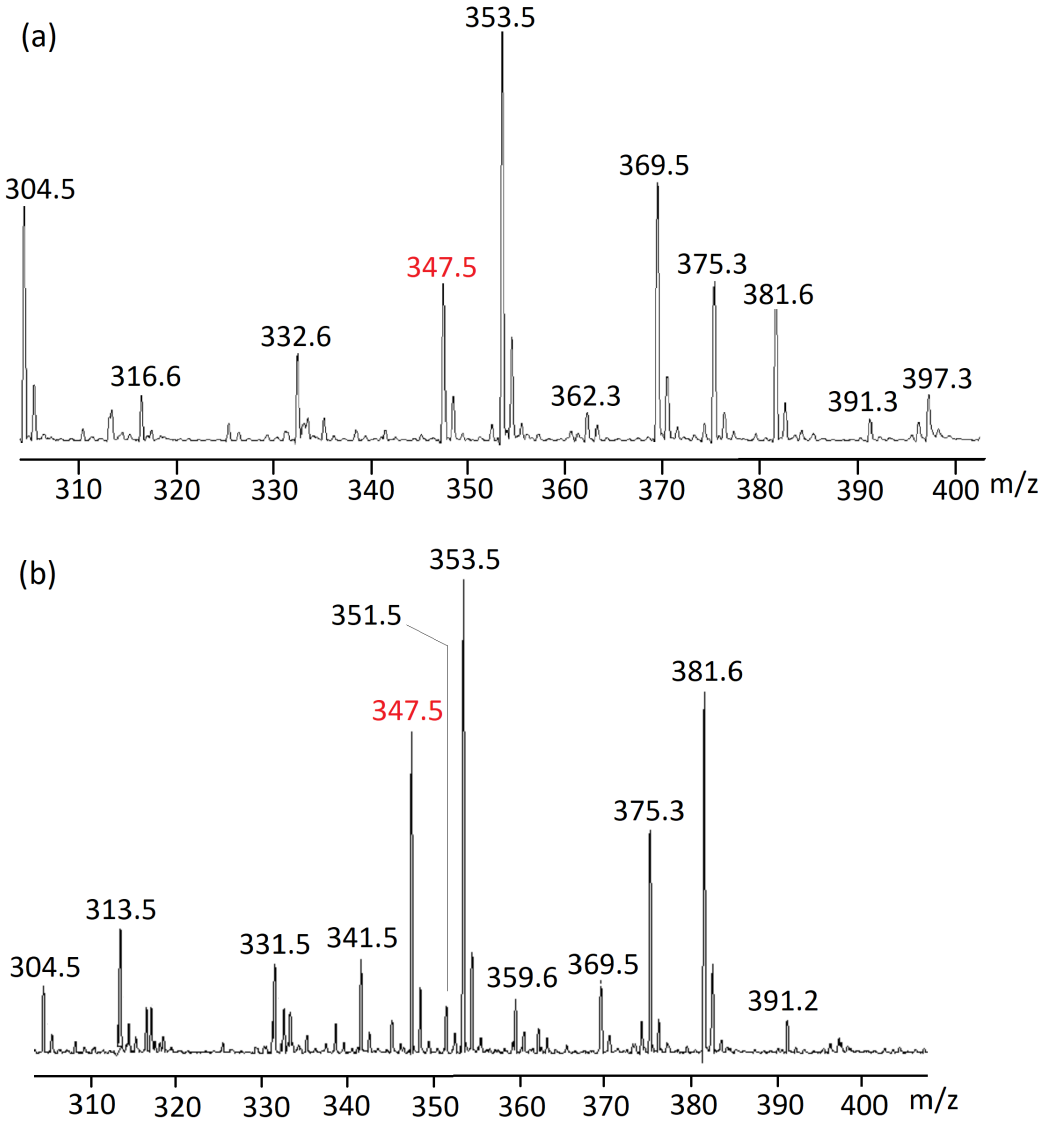

Figure 3.18: Positive ion MALDI TOF mass spectra of extracted turtle's plasma with added (a) corticosterone 2.5 mg/mL with DHB matrix and (b) corticosterone with 10 mg/mL labeled internal standard of final concentration 2.5 mg/mL with DHB matrix.

Figure 3.19 shows mass spectra of extracted turtle's plasma with added 2.5 mg/mL corticosterone acquired with sDHB matrix and spiked with IS. Signal at m/z 347.4 is easy detectable for both spectra, the signal at m/z 347.5 surpass other signals when spiked with IS. Background noise is negligible.

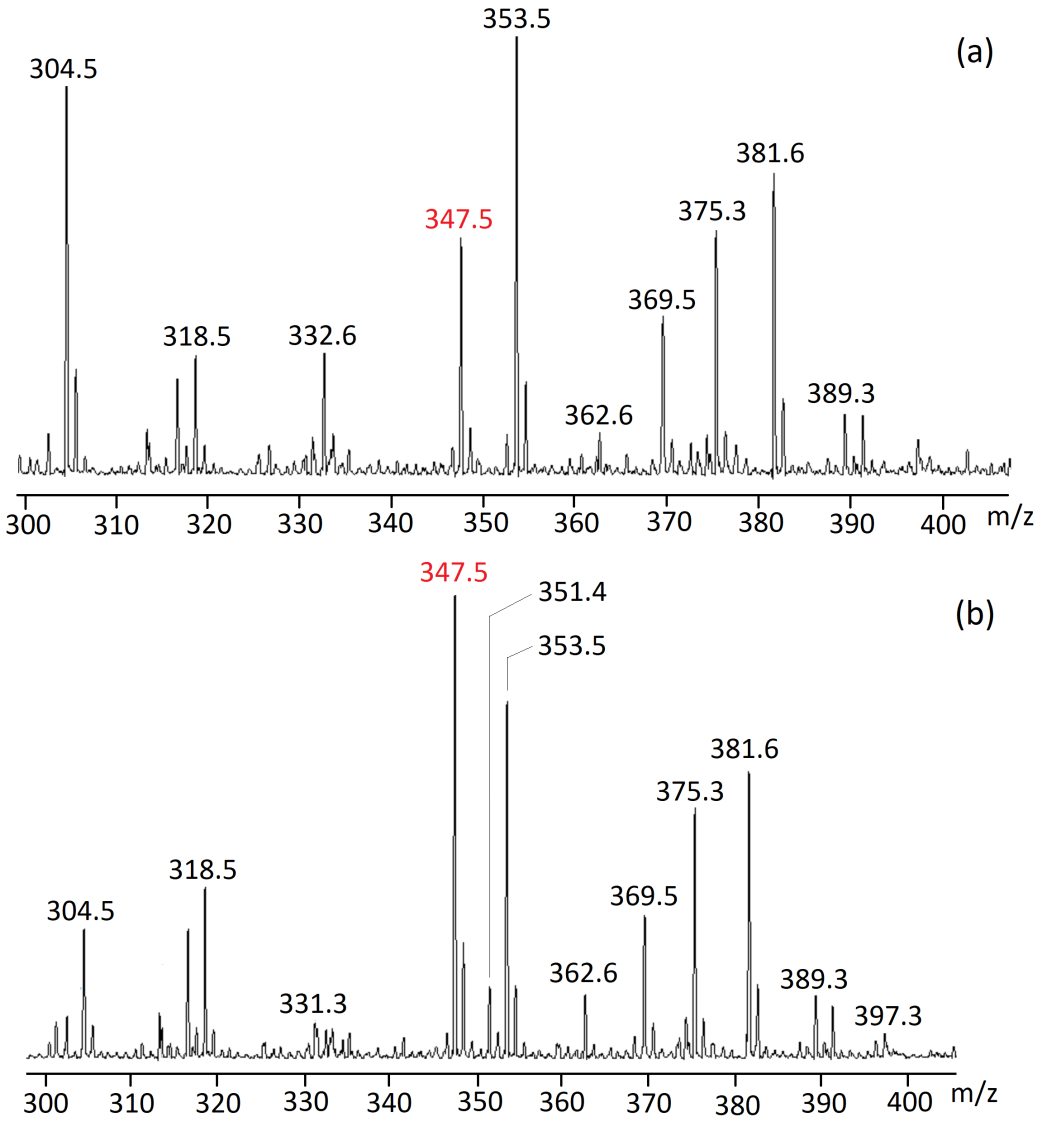

Figure 3.19: Positive ion MALDI TOF mass spectra of extracted turtle's plasma with added (a) corticosterone 2.5 mg/mL with sDHB matrix and (b) corticosterone with 10 mg/mL labeled internal standard of final concentration 2.5 mg/mL with sDHB matrix.

Table 3.8 shows the values for the limit of detection (LOD), the limit of quantification (LOQ), coefficient of determination (R^2). The values represent statistically processed S/N values detected in the plasma corticosterone spectra acquired with different matrices. Insufficient number of data was obtained for detailed regression analysis in the samples acquired with CHCA, therefore LOD, LOQ and R^2 are not given for each days. It might be due to the intensity of CHCA derived signals, and possibly the addition of new signals arising from the compounds co-extracted from the plasma with CS [78], thus yielding high intensity signals in the low mass region, which might lead to the suppression of extracted CS-derived signals. The same behaviour was observed also in the Figure 3.15, S/N values of CS in CHCA matrix are much lower compared to the DHB and sDHB matrix. The summary of day 1-3 of plasma sample without IS for CHCA matrix shows statistical significance and the limit of detection is 0.71, the limit of quantification is 2.36 and R^2 is 0.910, however it is not possible to compare with samples spiked with IS. The lowest value of LOD (0.04) was found for DHB matrix at day 1, followed by day 2 (0.07) and day 3 (0.07). The lowest value of LOQ (0.12) was found for DHB matrix at day 1. The limit of detection and limit of quantitation for DHB matrix summary of day 1-3 were 0.06 and 0.21, respectively. In case of DHB matrix the LOD and LOQ are higher when plasma sample was spiked with IS. The lowest value of LOD (0.11) when sDHB matrix was used was found at day 3. The results in case of sDHB matrix do not show regular pattern. The limit of detection and limit of quantitation for sDHB matrix summary of day 1-3 were 0.99 and 3.22, respectively, for samples spiked with IS are the values lower, 0.46 and 1.55, respectively. Lower LOD and LOQ values were obtained in the absence of IS when CS was extracted from plasma, compared to the model system tested in the first part of our work. For both matrices the coefficient of determination values are higher when IS was not used, either way, the results show good linearity of the measurement characteristic. Summary of day 1-3 for DHB matrix without IS ($R^2 = 0.997$) and with IS ($R^2 = 0.983$), and for sDHB matrix without ($R^2 = 0.994$) and with IS ($R^2 = 0.949$). Table 3.9 shows the linear equation with determined values for slope and intercept for the S/N values of CS detected in spectra with addition of IS obtained with matrices CHCA, DHB and sDHB, for three consecutive days of measurements.

Analysis of variance (ANOVA) was used to investigate and evaluate the relative quantification capacity and accuracy of developed method. Determination of the precision of analytical method is separated into within-run repeatability during one day of measurements and between day repeatability during three days and subsequently statistically processed. The values for the day-to-day repeatability and within day precision are given in Table

N_o Day	S/N	parameters	CHCA	DHB	sDHB
D1	347	LOD	-	0.04	2.09
		LOQ	-	0.12	6.97
		R^2	-	0.999	0.971
	347/351	LOD	-	0.17	0.60
		LOQ	-	0.57	1.99
		R^2	-	0.998	0.971
D2	347	LOD	-	0.07	0.98
		LOQ	-	0.25	3.27
		R^2	-	0.996	0.993
	347/351	LOD	-	1.18	0.84
		LOQ	-	3.93	2.80
		R^2	-	0.898	0.885
D3	347	LOD	-	0.07	0.11
		LOQ	-	0.24	0.36
		R^2	-	0.997	0.999
	347/351	LOD	-	0.46	0.78
		LOQ	-	1.55	2.59
		R^2	-	0.983	0.976
D1-D3	347	LOD	0.71	0.06	0.99
		LOQ	2.36	0.21	3.22
		R^2	0.910	0.997	0.994
	347/351	LOD	-	0.46	0.46
		LOQ	-	1.53	1.55
		R^2	-	0.983	0.949

Table 3.8: The calculated values (ANOVA analysis, regression) for the limit of detection (LOD), limit of quantification (LOQ) and coefficient of determination (R squared, R^2), for the S/N values (signals at m/z 347.4 and ration between signals at m/z 347.4 and at m/z 351.4) of CS detected in spectra with addition of IS obtained with matrices CHCA, DHB and sDHB, for three consecutive days of measurements.

N_o Day	S/N	CHCA	DHB	sDHB
D1	347	-	y=314.51x+13.65	y=20.79x+17.30
	347/351	-	y=3.52x–0.03	y=3.99x-0.16
D2	347	-	y=545.08x+22.66	y=19.29x+32.65
	347/351	-	y=2.31x+0.24	y=3.32x-0.28
D3	347	-	y=363.78x+44.28	y=27.53x+26.13
	347/351	-	y=2.43x+0.08	y=2.87x+0.29
D1-D3	347	y=22.77x+25.96	y=407.79x+26.86	y=22.54x+25.36
	347/351	-	y=2.76x+0.098	y=3.32x-0.05

Table 3.9: The linear equation with determined values for slope and intercept, for the S/N values (signals at m/z 347.4 and ration between signals at m/z 347.4 and at m/z 351.4) of CS detected in spectra with addition of IS obtained with matrices CHCA, DHB and sDHB, for three consecutive days of measurements.

3.10. Mean S/N values were calculated based on quadruplicate for all CS samples without and with IS and measurements during three days, for each applied matrices and six different concentrations in range from 39 μg/mL to 5 mg/mL. In red are given values below 15%. When CHCA was used as a matrix, the values of day-to-day reproducibility and within day precision always exceeded 15% and for some concentrations it was not possible to obtain statistical significance. Accordingly, CHCA is not a suitable matrix for analysis of corticosterone in plasma sample. The lowest value (3.15%) was find for DHB matrix, CS 1.25 mg/mL spiked with IS, day to day measurements, however, the same concentration when not spiked with IS shows high values (52.63%). The results do not show a uniform patter, nevertheless in most cases the values are lower when CS is spiked with IS. Within day measurements with sDHB matrix demonstrate reasonable results across all concentrations with and without IS, four of tested concentrations spiked with IS reached values below 15% and all of the concentrations with and without IS have values below 30%. The reproducibility of the method is reasonable and there exists potential for the quantitative analysis, however some improvements are necessary.

Table 3.11 lists the F and F critical values, acquired with ANOVA tools for signals at m/z 347.4 and ration between signals at m/z 347.4 and at m/z 351.4 of CS in plasma samples detected in spectra obtained without and with IS in range of concentrations from 39 μg/mL to 5 mg/mL. F values were calculated by ANOVA test in Excel program. F critical values (Fcrit) are determined from the statistical tables, which represent the upper critical values of the F distribution with the precision degree 95% and the factor α=0.05 for certain

mg		**ANOVA Day to day, %** *CHCA*	*DHB*	*sDHB*	**ANOVA Within day, %** *CHCA*	*DHB*	*sDHB*
0.039	347	40.35	41.83	33.97	53.98	20.66	23.38
	347/351	-	26.40	5.85	-	14.42	10.32
0.16	347	38.90	26.92	15.26	77.91	16.80	15.90
	347/351	-	10.08	14.99	-	15.48	12.62
0.6	347	31.12	29.42	84.76	90.85	20.35	21.36
	347/351	36.75	45.16	44.38	15.32	5.40	8.37
1.25	347	60.44	52.63	84.88	25.14	20.71	29.72
	347/351	-	3.15	12.99	-	6.40	21.95
2.5	347	67.68	37.29	61.22	40.58	36.06	26.49
	347/351	-	27.10	32.56	-	21.32	29.77
5.0	347	29.34	6.94	11.30	45.17	12.26	26.51
	347/351	22.43	80.23	131.94	119.77	27.27	13.18

Table 3.10: The values of day to day repeatability and within day precision, calculated with ANOVA tools, for the mean S/N values (signals at m/z 347.4 and ration between signals at m/z 347.4 and at m/z 351.4) of CS in plasma samples detected in spectra acquired without and with IS with different concentrations, and with three different matrices CHCA, DHB and sDHB. In red are values below 15.

mg		**F** *CHCA*	*DHB*	*sDHB*	**Fcrit** *CHCA*	*DHB*	*sDHB*
0.039	347	2.68	13.30	7.33	10.33	4.26	5.14
	347/351	-	11.05	1.96	-	4.74	10.13
0.16	347	0.25	8.70	3.76	10.13	4.26	4.26
	347/351	-	2.27	5.23	-	4.46	4.74
0.6	347	0.65	7.27	48.25	5.14	4.26	4.26
	347/351	18.26	211.43	85.34	10.13	4.26	5.99
1.25	347	18.33	20.37	25.46	161.45	5.99	4.74
	347/351	-	0.27	2.05	-	4.46	4.26
2.5	347	9.34	4.21	17.03	18.51	4.26	4.74
	347/351	-	5.85	4.59	-	4.26	4.74
5.0	347	2.27	0.04	1.55	4.74	5.99	4.26
	347/351	0.89	26.97	301.65	6.94	4.46	5.99

Table 3.11: The F and F critical values, calculated with ANOVA tools for signals at m/z 347.4 and ration between signals at m/z 347.4 and at m/z 351.4 of CS in plasma samples detected in spectra acquired without and with IS with different concentrations. The red color indicates the values when F is higher than F critical.

number of measurements. Values written in red indicate that F is higher than Fcrit, or the variations in groups have significant differences, and they are higher than variations between groups, the null hypothesis is rejected and the mean values are not equal. Higher value of F, bigger differences between groups. Not all of the values were obtained when CHCA matrix was used, the detectability was not good or the signal was detected in 1 of 4 wells. Fcrit values for DHB and sDHB matrices have regular pattern within all tested concentrations, whereas F values differs significantly.

Chapter 4

Conclusions

In this study, it was demonstrated that MALDI mass spectrometry has the potential for the evaluation of stress level in turtles based on the determination of corticosterone level in blood. Along with advantages, such as the speed of analysis and parameters that can be used for quantitation, tested approach has an of limitations, mostly related to the sensitivity of CS detection, but in terms of precision and accuracy it is worth of considerations for further improvements. The detection of CS in the physiological solution was possible, by suggested the MALDI TOF MS approach and using CHCA matrix,. However, the lowest concentration of CS extracted from plasma that was still detectable by MALDI TOF MS was about 0.04 mg/mL, which is about ten times higher than expected CS concentration in a blood. The best results was obtained with the DHB matrix.

Results obtained in this study demonstrate the following:

- In spite of drawbacks of MALDI for detection and analysis of low mass molecules, it is possible to detect cholesterol by MALDI-TOF MS with DHB and sDHB matrices. Compared to DHB matrix, the sDHB matrix has achieved higher S/N for the cholesterol-related signal.

- Nanoparticles, CDs or N-CDs, are not suitable for detection of cholesterol by MALDI MS, but their addition to the organic matrices helps to overcome the signal suppression caused by the presence of inorganic salts, such as NaCl.

- A binary system made from graphene and sDHB matrix showed the highest efficiency as a matrix at higher concentrations of cholesterol, nevertheless with a decrease of concentration the detection was not possible anymore, therefore this conjunction is inapplicable as for hormones detection is required high sensitivity.

- The MALDI TOF MS method for quantification of corticosterone in physiological solution was developed and it involves the application of the internal standard that results in better reproducibility and precision of the data obtained. The best sensitivity was obtained by using CHCA matrix, whereas the other two matrices showed also promising results.

- Finally, detection of CS in the blood without and with extraction was not possible, most likely due to interference of other compounds present in the blood/extraction of the mixture, which decreases the sensitivity of this approach. There is also a question of CS concentration in the blood of an individual turtle and the extraction efficiency, but this is beyond the topic of this study.

In summary, due to the advantages presented in this study, it is suggested that MALDI TOF mass spectrometric approach has a great potential for the evaluation of CS in blood, and that the method could be applied also for analysis of another biologically relevant low mass molecules.

References

[1] Dimitris Margaritoulis et al. "Loggerhead turtles in the Mediterranean: present knowledge and conservation perspectives". In: *Loggerhead Sea Turtles (editors: AB Bolten and BE Witherington). Smithsonian Institution Press, Washington, DC, USA* (2003), pp. 175–198.

[2] Pamela T Plotkin and James R Spotila. "Post-nesting migrations of loggerhead turtles Caretta caretta from Georgia, USA: conservation implications for a genetically distinct subpopulation". In: *Oryx* 36.4 (2002), pp. 396–399.

[3] Karen A Bjorndal et al. "Compensatory growth in oceanic loggerhead sea turtles: response to a stochastic environment". In: *Ecology* 84.5 (2003), pp. 1237–1249.

[4] B Witherington. "Ecology of neonate loggerhead turtles inhabiting lines of downwelling near a Gulf Stream front". In: *Marine Biology* 140.4 (2002), pp. 843–853.

[5] Alan B Bolten et al. "Size distribution of pelagic-stage loggerhead sea turtles (Caretta caretta) in the waters around the Azores and Madeira". In: *ARQUIPÉLAGO. Ciências Biológicas e Marinhas= Life and Marine Sciences* 11 (1993), pp. 49–54.

[6] Alan B Bolten et al. "Size distribution of pelagic-stage loggerhead sea turtles (Caretta caretta) in the waters around the Azores and Madeira". In: *ARQUIPÉLAGO. Ciências Biológicas e Marinhas= Life and Marine Sciences* 11 (1993), pp. 49–54.

[7] Alan B Bolten et al. "Transatlantic developmental migrations of loggerhead sea turtles demonstrated by mtDNA sequence analysis". In: *Ecological Applications* 8.1 (1998), pp. 1–7.

[8] Carla Freitas, Rui Caldeira, and Thomas Dellinger. "Surface behavior of pelagic juvenile loggerhead sea turtles in the eastern North Atlantic". In: *Journal of experimental marine biology and ecology* 510 (2019), pp. 73–80.

[9] Ilaria Caliani et al. “An immune response-based approach to evaluate physiological stress in rehabilitating loggerhead sea turtle”. In: *Veterinary Immunology and Immunopathology* 207.June 2018 (2019), pp. 18–24. ISSN: 18732534. DOI: 10.1016/j.vetimm.2018.11.013. URL: https://doi.org/10.1016/j.vetimm.2018.11.013.

[10] Deborah T Crouse, Larry B Crowder, and Hal Caswell. “A stage-based population model for loggerhead sea turtles and implications for conservation”. In: *Ecology* 68.5 (1987), pp. 1412–1423.

[11] Alan B Bolten and Blair E Witherington. “Loggerhead sea turtles”. In: *Marine Turtle Newsl* 104 (2004), p. 319.

[12] RE Wolke, DR Brooks, and A George. “Spirorchidiasis in loggerhead sea turtles (Caretta caretta): pathology”. In: *Journal of Wildlife Diseases* 18.2 (1982), pp. 175–185.

[13] Ana Luisa Valente et al. “Helminth component community of the loggerhead sea turtle, Caretta caretta, from Madeira Archipelago, Portugal”. In: *Journal of Parasitology* 95.1 (2009), pp. 249–252.

[14] ME Lutcavage and PL Lutz. “Diving physiology”. In: *The biology of sea turtles* 1 (1997), pp. 276–296.

[15] Robert Ader and Nicholas Cohen. “Psychoneuroimmunology: Conditioning and Stress”. In: *Annual Review of Psychology* 44 (1 Jan. 1993), pp. 53–85. ISSN: 0066-4308. DOI: 10.1146/annurev.ps.44.020193.000413. URL: http://www.annualreviews.org/doi/10.1146/annurev.ps.44.020193.000413.

[16] PL Lutz. “Health related sea turtle physiology”. In: *Report of the Sea Turtle Health Assessment Workshop*. US Department of Commerce, NOAA Technical Memorandum NOS-NCCOS-CCEHBR-0003. 1998, pp. 45–49.

[17] Molly E Lutcavage. “Human impacts on sea turtle survival”. In: *The Biology of Sea Turtles, Volume I*. CRC press, 2017, pp. 387–409.

[18] Christopher K Pham et al. “Plastic ingestion in oceanic-stage loggerhead sea turtles (Caretta caretta) off the North Atlantic subtropical gyre”. In: *Marine pollution bulletin* 121.1-2 (2017), pp. 222–229.

[19] National Research Council et al. *Decline of the sea turtles: causes and prevention*. National Academies Press, 1990.

[20] Dayton L Alverson et al. *A global assessment of fisheries bycatch and discards*. Vol. 339. Food & Agriculture Org., 1994.

[21] Erika A Zollett. "Bycatch of protected species and other species of concern in US east coast commercial fisheries". In: *Endangered Species Research* 9.1 (2009), pp. 49–59.

[22] Dale Squires et al. "Fisheries bycatch reduction within the least-cost biodiversity mitigation hierarchy: Conservatory offsets with an application to sea turtles". In: *Marine Policy* 93 (2018), pp. 55–61. ISSN: 0308-597X. DOI: https://doi.org/10.1016/j.marpol.2018.03.018. URL: https://www.sciencedirect.com/science/article/pii/S0308597X17303020.

[23] Kimberly A. Riskas, Mariana M.P.B. Fuentes, and Mark Hamann. "Justifying the need for collaborative management of fisheries bycatch: A lesson from marine turtles in Australia". In: *Biological Conservation* 196 (2016), pp. 40–47. ISSN: 0006-3207. DOI: https://doi.org/10.1016/j.biocon.2016.02.001. URL: https://www.sciencedirect.com/science/article/pii/S0006320716300349.

[24] Filipa Pinho Duarte. "Reavaliação da captura acidental de tartarugas marinhas na Região Autónoma da Madeira". MA thesis. Universidade de Évora, 2021.

[25] HPO Encarnação. "Captura acidental de tartarugas marinhas pela frota de pesca madeirense". In: *Relatório de Estágio do Curso de Biologia, Universidade da Madeira, Funchal* (1998).

[26] RL Ferreira et al. "Influence of environmental and fishery parameters on loggerhead sea turtle by-catch in the longline fishery in the Azores archipelago and implications for conservation". In: *Marine Biological Association of the United Kingdom. Journal of the Marine Biological Association of the United Kingdom* 91.8 (2011), p. 1697.

[27] Rebecca L Lewison, Sloan A Freeman, and Larry B Crowder. "Quantifying the effects of fisheries on threatened species: the impact of pelagic longlines on loggerhead and leatherback sea turtles". In: *Ecology letters* 7.3 (2004), pp. 221–231.

[28] DR Clark Jr and AJ Krynitsky. "Organochlorine residues in eggs of loggerhead and green sea turtles nesting at Merritt Island, Florida–July and August 1976." In: *Pesticides Monitoring Journal* 14.1 (1980), pp. 7–10.

[29] Clevo Wilson and Clem Tisdell. "Conservation and economic benefits of wildlife-based marine tourism: sea turtles and whales as case studies". In: *Human Dimensions of Wildlife* 8.1 (2003), pp. 49–58.

[30] Clement Allan Tisdell and Clevo Wilson. "Does tourism contribute to sea turtle conservation". In: *Is the flagship status of turtles advantageous* (2005), pp. 145–167.

[31] Bernard Devaux and Bernard De Wetter. *On the trail of sea turtles*. Barron's Educational Series, 2000.

[32] Clem Tisdell and Clevo Wilson. "Economic, educational and conservation benefits of sea turtle based ecotourism". In: *Sustainable Tourism Cooperative Research Centre, Gold Coast* (2002).

[33] Assembleia Regional da Madeira. "Decreto Legislativo Regional n.º 18/85/M de 7 de Setembro: Protecção das tartarugas marinhas." In: *Diário da República* ***I Série*** *(206), 2912* (1985), [**PDF**].

[34] Assembleia Regional da Madeira. "Decreto Legislativo Regional n.º 15/2013/M de 14 de maio: Aprova o Regulamento da Atividade de Observação de Vertebrados Marinhos na Região Autónoma da Madeira." In: *Jornal Oficial da Região Autónoma da Madeira* ***I Série*** *(57)* (2013), 2–12., [**PDF**].

[35] Antonino Pace et al. "Loggerhead sea turtles as sentinels in the western mediterranean: Antibiotic resistance and environment-related modifications of gram-negative bacteria". In: *Marine pollution bulletin* 149 (2019), p. 110575.

[36] European Parliament & Council of the European Union. "Directive 2008/56/EC of 17 June 2008 establishing a framework for community action in the field of marine environmental policy (Marine Strategy Framework Directive)." In: *Official Journal of the European Union EN* ***L 164*** *(25.6.2008)* 25 June 2008 (2008), 19–40. [**PDF**].

[37] Lisa F Gregory and Jeffrey R Schmid. "Stress responses and sexing of wild Kemp's ridley sea turtles (Lepidochelys kempii) in the northeastern Gulf of Mexico". In: *General and Comparative Endocrinology* 124.1 (2001), pp. 66–74.

[38] Lisa F Gregory et al. "Plasma corticosterone concentrations associated with acute captivity stress in wild loggerhead sea turtles (Caretta caretta)". In: *General and comparative endocrinology* 104.3 (1996), pp. 312–320.

[39] Z. Mack and H. B. Fokidis. "A novel method for assessing chronic cortisol concentrations in dogs using the nail as a source". In: *Domestic Animal Endocrinology* 59 (2017), pp. 53–57. ISSN: 07397240. DOI: 10.1016/j.domaniend.2016.11.003. URL: http://dx.doi.org/10.1016/j.domaniend.2016.11.003.

[40] William B. Cash, Rebecca L. Holberton, and Scott S. Knight. "Corticosterone secretion in response to capture and handling in free- living red-eared slider turtles". In: *General and Comparative Endocrinology* 108.3 (1997), pp. 427–433. ISSN: 10956840. DOI: 10.1006/gcen.1997.6999.

[41] A Ghulam et al. "Quantitative analysis of human serum corticosterone by high-performance liquid chromatography coupled to electrospray ionization mass spectrometry". In: *Journal of Chromatography B: Biomedical Sciences and Applications* 727.1-2 (1999), pp. 227–233.

[42] Martin Fenske. "Determination of cortisol in human plasma by thin-layer chromatography and fluorescence derivatization with isonicotinic acid hydrazide". In: *Journal of Chromatographic Science* 46.1 (2008), pp. 1–3. ISSN: 00219665. DOI: 10.1093/chromsci/46.1.1.

[43] Ming-Hui Yang et al. "Quantitative analysis of progesterone using isotope dilution-matrix-assisted laser desorption ionization-time of flight mass spectrometry as a reference procedure for radioimmunoassay". In: *Clinica Chimica Acta* 512 (2021), pp. 106–111. ISSN: 0009-8981. DOI: https://doi.org/10.1016/j.cca.2019.11.020. URL: https://www.sciencedirect.com/science/article/pii/S0009898119321424.

[44] Hao Yang Wang et al. "Analysis of low molecular weight compounds by MALDI-FTICR-MS". In: *Journal of Chromatography B: Analytical Technologies in the Biomedical and Life Sciences* 879.17-18 (2011), pp. 1166–1179. ISSN: 15700232. DOI: 10.1016/j.jchromb.2011.03.037. URL: http://dx.doi.org/10.1016/j.jchromb.2011.03.037.

[45] Ignacy Rzagalinski and Dietrich A. Volmer. "Quantification of low molecular weight compounds by MALDI imaging mass spectrometry – A tutorial review". In: *Biochimica et Biophysica Acta - Proteins and Proteomics* 1865.7 (2017), pp. 726–739. ISSN: 18781454. DOI: 10.1016/j.bbapap.2016.12.011. URL: http://dx.doi.org/10.1016/j.bbapap.2016.12.011.

[46] Suming Chen et al. "Carbon nanodots as a matrix for the analysis of low-molecular-weight molecules in both positive- and negative-ion matrix-assisted laser desorption/ionization time-of-flight mass spectrometry and quantification of glucose and uric acid in real samples". In: *Analytical Chemistry* 85.14 (2013), pp. 6646–6652. ISSN: 00032700. DOI: 10.1021/ac401601r.

[47] William D. Blincoe et al. “Practical guide on MALDI-TOF MS method development for high throughput profiling of pharmaceutically relevant, small molecule chemical reactions”. In: *Tetrahedron* 76.36 (2020), p. 131434. ISSN: 14645416. DOI: 10.1016/j.tet.2020.131434. URL: https://doi.org/10.1016/j.tet.2020.131434.

[48] Masanobu Nishidate et al. “Applications of MALDI mass spectrometry imaging for pharmacokinetic studies during drug development”. In: *Drug Metabolism and Pharmacokinetics* 34.4 (2019), pp. 209–216. ISSN: 18800920. DOI: 10.1016/j.dmpk.2019.04.006. URL: https://doi.org/10.1016/j.dmpk.2019.04.006.

[49] Mohammed A. Meetani et al. “Desorption electrospray ionization mass spectrometry of intact bacteria”. In: *Journal of Mass Spectrometry* 42.9 (2007), pp. 1186–1193. ISSN: 10765174. DOI: 10.1002/jms.1250.

[50] Antony Croxatto, Guy Prod’hom, and Gilbert Greub. “Applications of MALDI-TOF mass spectrometry in clinical diagnostic microbiology”. In: *FEMS Microbiology Reviews* 36.2 (2012), pp. 380–407. ISSN: 01686445. DOI: 10.1111/j.1574-6976.2011.00298.x.

[51] Yi Chi Ho et al. “Nanoparticle-assisted MALDI-TOF MS combined with seed-layer surface preparation for quantification of small molecules”. In: *Analytica Chimica Acta* 697.1-2 (2011), pp. 1–7. ISSN: 00032670. DOI: 10.1016/j.aca.2011.04.008. URL: http://dx.doi.org/10.1016/j.aca.2011.04.008.

[52] “Detection of small molecules using SBA-15 modified CHCA as a novel matrix of MALDI-TOF MS”. In: *International Journal of Mass Spectrometry* 417.1 (2017), pp. 34–39. ISSN: 13873806. DOI: 10.1016/j.ijms.2017.04.004. URL: http://dx.doi.org/10.1016/j.ijms.2017.04.004.

[53] Sumeyra Savas et al. “From days to hours: Can MALDI-TOF MS system replace both conventional and molecular typing methods with new cut off level for Vancomycin Resistant Enterococcus faecium”. In: *Journal of Microbiological Methods* 162.December 2018 (2019), pp. 62–68. ISSN: 18728359. DOI: 10.1016/j.mimet.2018.12.015. URL: https://doi.org/10.1016/j.mimet.2018.12.015.

[54] Cosima Damiana Calvano et al. “MALDI matrices for low molecular weight compounds: an endless story?” In: *Analytical and bioanalytical chemistry* 410.17 (2018), pp. 4015–4038.

[55] Hong zhi Tang et al. "Detection of small molecules using SBA-15 modified CHCA as a novel matrix of MALDI-TOF MS". In: *International Journal of Mass Spectrometry* 417.1 (2017), pp. 34–39. ISSN: 13873806. DOI: 10.1016/j.ijms.2017.04.004. URL: http://dx.doi.org/10.1016/j.ijms.2017.04.004.

[56] Bruker. "Instructions for Use - Bruker Guide to MALDI Sample Preparation - Revision E". In: December (2015), pp. 1–15. URL: www.bruker.com/care.

[57] Kevin M. McAvey et al. "Laser-induced oxidation of cholesterol observed during MALDI-TOF mass spectrometry". In: *Journal of the American Society for Mass Spectrometry* 22.4 (2011), pp. 659–669. ISSN: 10440305. DOI: 10.1007/s13361-011-0074-3.

[58] Shu Zhang et al. "A Novel Strategy for MALDI-TOF MS Analysis of Small Molecules". In: *Journal of the American Society for Mass Spectrometry* 21.1 (2010), pp. 154–160. ISSN: 10440305. DOI: 10.1016/j.jasms.2009.09.024. URL: http://dx.doi.org/10.1016/j.jasms.2009.09.024.

[59] Paulina Kobylis, Piotr Stepnowski, and Magda Caban. "Review of the applicability of ionic liquid matrices for the quantification of small molecules by MALDI MS". In: *Microchemical Journal* 164 (2021), p. 105983. ISSN: 0026-265X. DOI: https://doi.org/10.1016/j.microc.2021.105983. URL: https://www.sciencedirect.com/science/article/pii/S0026265X21000680.

[60] Li-Kang Zhang and Michael L Gross. "Location of abasic sites in oligodeoxynucleotides by tandem mass spectrometry and by a chemical cleavage initiated by an unusual reaction of the ODN with MALDI matrix". In: *Journal of the American Society for Mass Spectrometry* 13.12 (2002), pp. 1418–1426.

[61] MS Slyundina et al. "Tryptamine: a reactive matrix for MALDI mass spectrometry". In: *Journal of analytical chemistry* 72.13 (2017), pp. 1295–1299.

[62] Rui Chen et al. "High-salt-tolerance matrix for facile detection of glucose in rat brain microdialysates by maldi mass spectrometry". In: *Analytical Chemistry* 84.1 (2012), pp. 465–469. ISSN: 00032700. DOI: 10.1021/ac202438a.

[63] Shuping Long et al. “Nanoporous silica coupled MALDI-TOF MS detection of Bence-Jones proteins in human urine for diagnosis of multiple myeloma”. In: *Talanta* 200.December 2018 (2019), pp. 288–292. ISSN: 00399140. DOI: 10.1016/j.talanta.2019.03.067. URL: https://doi.org/10.1016/j.talanta.2019.03.067.

[64] Mei Chun Tseng et al. “Dihydrobenzoic acid modified nanoparticle as a MALDI-TOF MS matrix for soft ionization and structure determination of small molecules with diverse structures”. In: *Journal of the American Society for Mass Spectrometry* 21.11 (2010), pp. 1930–1939. ISSN: 10440305. DOI: 10.1016/j.jasms.2010.08.001. URL: http://dx.doi.org/10.1016/j.jasms.2010.08.001.

[65] Dominika Houdova et al. “Cholesterol Detection by MALDI TOF mass spectrometry .” In: *Journal of Colloid and Interface Science* (2021). ISSN: 0021-9797. DOI: 10.1016/j.jcis.2021.02.004. URL: https://www.sciencedirect.com/science/article/abs/pii/S0021979721001338.

[66] “Big molecule ejection - SIMS vs. MALDI”. In: *Applied Surface Science* 203-204 (2003), pp. 69–71. ISSN: 01694332. DOI: 10.1016/S0169-4332(02)00661-X.

[67] “Desorption/ionization of molecular nanoclusters: SIMS versus MALDI”. In: *Applied Surface Science* 231-232 (2004), pp. 131–135. ISSN: 01694332. DOI: 10.1016/j.apsusc.2004.03.092.

[68] Yi Shan Li, Wei Lung Tseng, and Chi Yu Lu. “Sensitive detection of quinoline-derivatized sitagliptin in small volumes of human plasma by MALDI-TOF mass spectrometry”. In: *Talanta* 218.May (2020), p. 121143. ISSN: 00399140. DOI: 10.1016/j.talanta.2020.121143. URL: https://doi.org/10.1016/j.talanta.2020.121143.

[69] Anping Xu et al. “Evaluation of MALDI-TOF MS for the measurement of glycated hemoglobin”. In: *Clinica Chimica Acta* 498.1120 (2019), pp. 154–160. ISSN: 18733492. DOI: 10.1016/j.cca.2019.08.025. URL: https://doi.org/10.1016/j.cca.2019.08.025.

[70] Fawzi A. El-Yazbi et al. “A novel voltammetry offline coupled MALDI/TOF MS characterization of electrochemical reaction products and the voltammetric determination of febuxostat in human plasma”. In: *Talanta* 194.October 2018 (2019), pp. 542–547. ISSN: 00399140. DOI: 10.1016/j.talanta.2018.10.087. URL: https://doi.org/10.1016/j.talanta.2018.10.087.

[71] Jitender Bariwal and Erik Van Der Eycken. "C-N bond forming cross-coupling reactions: An overview". In: *Chemical Society Reviews* 42.24 (2013), pp. 9283–9303. ISSN: 14604744. DOI: 10.1039/c3cs60228a.

[72] Ambrose Furey et al. "Ion suppression; A critical review on causes, evaluation, prevention and applications". In: *Talanta* 115 (2013), pp. 104–122. ISSN: 00399140. DOI: 10.1016/j.talanta.2013.03.048. URL: http://dx.doi.org/10.1016/j.talanta.2013.03.048.

[73] Chensong Pan et al. "Using oxidized carbon nanotubes as matrix for analysis of small molecules by MALDI-TOF MS". In: *Journal of the American Society for Mass Spectrometry* 16.6 (2005), pp. 883–892. ISSN: 10440305. DOI: 10.1016/j.jasms.2005.03.009.

[74] Shu Zhang et al. "New matrix of MALDI-TOF MS for analysis of small molecules". In: *Chinese Chemical Letters* 20.12 (2009), pp. 1495–1497. ISSN: 10018417. DOI: 10.1016/j.cclet.2009.06.031.

[75] I Popović et al. "TiO 2 nanocrystals–assisted laser desorption and ionization time-of-flight mass spectrometric analysis of steroid hormones, amino acids and saccharides. Validation and comparison of methods". In: *RSC advances* 6.2 (2016), pp. 1027–1036.

[76] BB Campos et al. "Fluorescent chemosensor for pyridine based on N-doped carbon dots". In: *Journal of colloid and interface science* 458 (2015), pp. 209–216.

[77] S Benard et al. "Experiments towards quantification of saturated and polyunsaturated diacylglycerols by matrix-assisted laser desorption and ionization time-of-flight mass spectrometry". In: *Chemistry and Physics of Lipids* 100.1 (1999), pp. 115–125. ISSN: 0009-3084. DOI: https://doi.org/10.1016/S0009-3084(99)00045-6. URL: https://www.sciencedirect.com/science/article/pii/S0009308499000456.

[78] Marijana Petković et al. "Performances of ionic liquid matrices with butyl ammonium counterion for matrix-assisted laser desorption/ionization mass spectrometric detection and analysis of sucralfate". In: *Journal of Carbohydrate Chemistry* 39.1 (2020), pp. 1–23.

Appendix

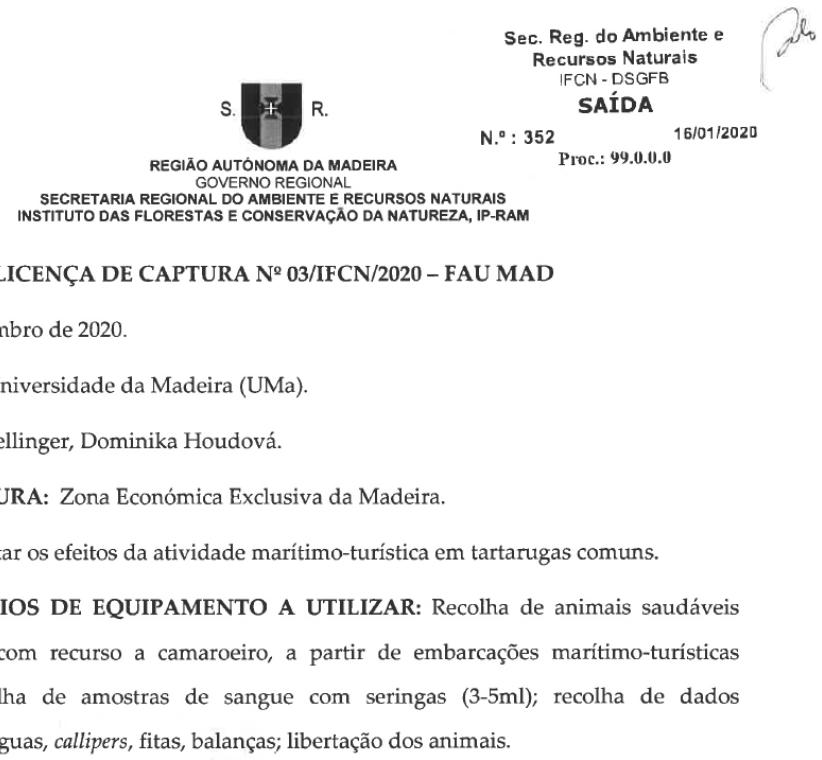

Sec. Reg. do Ambiente e
Recursos Naturais
IFCN - DSGFB
SAÍDA
N.º : 352 16/01/2020
Proc.: 99.0.0.0

S. R.

REGIÃO AUTÓNOMA DA MADEIRA
GOVERNO REGIONAL
SECRETARIA REGIONAL DO AMBIENTE E RECURSOS NATURAIS
INSTITUTO DAS FLORESTAS E CONSERVAÇÃO DA NATUREZA, IP-RAM

LICENÇA DE CAPTURA Nº 03/IFCN/2020 – FAU MAD

VALIDADE: dezembro de 2020.

INSTITUIÇÃO: Universidade da Madeira (UMa).

NOME: Thomas Dellinger, Dominika Houdová.

LOCAL DE CAPTURA: Zona Económica Exclusiva da Madeira.

FINALIDADE: testar os efeitos da atividade marítimo-turística em tartarugas comuns.

MÉTODOS E MEIOS DE EQUIPAMENTO A UTILIZAR: Recolha de animais saudáveis manualmente ou com recurso a camaroeiro, a partir de embarcações marítimo-turísticas colaborantes; recolha de amostras de sangue com seringas (3-5ml); recolha de dados biométricos com réguas, *callipers*, fitas, balanças; libertação dos animais.

Figure 4.1: Capture license N°03/IFCN/2020 - FAU MAD, page 1.

ESPÉCIES-ALVO: *Caretta caretta.*

NÚMERO DE ESPÉCIMES: Indeterminado (a constar em relatório final).

OBSERVAÇÕES:

1. O beneficiário desta licença deverá informar o Instituto das Florestas e Conservação da Natureza, IP-RAM dos contingentes de material efetivamente recolhido ao abrigo desta licença.
   Sim ☒ Não
2. Nas saídas de campo previstas, deverá o beneficiário fazer-se acompanhar obrigatoriamente de pessoal destacado para o efeito, nomeadamente guardas florestais, vigilantes da natureza e/ou técnicos do IFCN.
   Sim Não ☒
3. Os resultados dos estudos a realizar, bem como publicações decorrentes deste trabalho de campo deverão ser posteriormente enviados a este Instituto.
   Sim ☒ Não
4. Caso ocorra colheita de material, em relação a alguns exemplares, a mesma deverá ser em duplicado para entrega nas coleções do Jardim Botânico da Madeira.
   Sim Não ☒

Funchal, 16 de janeiro de 2020

O Diretor de Serviços

Região Autónoma da Madeira
Secretaria Regional do Ambiente e Recursos Naturais
Instituto das Florestas e Conservação da Natureza
Direção de Serviços de Gestão Florestal

Paulo Jorge Freitas

Quinta Vila Passos - Rua Alferes Veiga Pestana, 15 | 9054-505Funchal | T. +351 291 740 040/60
www.madeira.gov.pt | ifcn@madeira.gov.pt | NIF: 600086968

Figure 4.2: Capture license N°03/IFCN/2020 - FAU MAD, page 2.